Fermilab Proposal No. 383

Scientific Spokesman:
H.G.E.Kobrak
University of California,San Diego
(714) 452-3268
FTS Operator (714) 293-5000
At Fermilab ext.3056/4198

A PROPOSAL TO STUDY THE INCLUSIVE PRODUCTION OF K_S^o BY K^- ON HYDROGEN

H.G.E.Kobrak, R.E.Pitt, R.A.Swanson
University of California, San Diego
La Jolla, CA, 92037

February 1975

A PROPOSAL TO STUDY THE INCLUSIVE PRODUCTION OF K_S^o BY K^- ON HYDROGEN

ABSTRACT

We propose to measure the inclusive cross section $d^2\sigma/dxdt$ for the reaction $(K^-P) \Rightarrow (K_S^oX)$ with incident kaons of 20 to 150 GeV/c. The experiment is intended to study the triple Regge region of the x,t plane $(0.8 < x < 1,\ 0 < -t < 3)$ In this region we will be able to compare our results with triple Regge theory. By adding the constraints of SU_3 and factorization, we can make direct comparision with the production of π^o and η by π^-.

The K_S^o would be detected by the (π^+,π^-) decay in a pair spectrometer such as that used in the K_S^o regeneration experiment E-82. The experiment would be well suited for the proposed charged mode of the M4 beam line, where this spectrometer has already been used.

We expect to participate in the installation and tuneup of the new charged beam. This time is impossible to estimate because of access problems. Once the beam is ready, we request two separate running periods. 200 hours for setup and initial data taking, followed by a period of data analysis before a final run of 300 hours.

I. INTRODUCTION

A major part of high energy physics research is devoted to hadronic processes of the form

$$A + B \rightarrow A + B \qquad (1)$$

or their inclusive counterparts

$$A + B \rightarrow A + X \qquad (2)$$

One expects that both types of processes can be interpreted in terms of the exchange of Regge poles. Processes of type (1) can be described by direct Regge exchanges. The analysis of processes of type (2) is done through the Mueller generalized optical theorem [1], which relates the inclusive cross section $d^2\sigma/dtdx$ for (2) to the absorptive part of the three body process

$$A + B + \bar{A} \rightarrow A + B + \bar{A}$$

In the appropriate part of the x,t plane, the three body forward amplitude can be expressed in terms of Regge poles and triple Regge/Pomeron vertices; hence triple Regge theory [2].

The number of trajectories which contribute to (1) and (2) is enormous; in most cases any neutral non strange meson trajectory will do, such as P(Pomeron),P',π,ρ,ω,f,A_2. This leads to a very complex analysis in which it is difficult to draw conclusions regarding the contributions of individual trajectories[3].

One can create situations more amenable to analysis in one of two ways; by taking differences of cross sections for processes such as $(AB) \rightarrow (AB)$ and $(\bar{A}B) \rightarrow (\bar{A}B)$ or by studying processes which intrinsically select a small number of Regge poles. Examples of the latter are the coherent regeneration process $(K_L A) \rightarrow (K_S A)$ (Experiment 82) which is pure ω exchange if A

is an isotopic singlet (ω and ρ for other isotopic spins), and pion charge exchange $(\pi^- P) \rightarrow (\pi^0 N)$ (Experiment 111) which is pure ρ exchange.

We propose here to measure the inclusive production of $\overline{K^0}$ by K^- in hydrogen $(K^- P) \rightarrow (\overline{K^0} X)$. This process should invole only ρ and A_2 exchange, which implies a relatively simple situation for analysis by Regge theory. We are further motivated by the existence of Experiment 350, which will measure inclusive production of π^0 and η by π^- on hydrogen. By invoking SU_3 and factorization of Regge amplitudes, we will be able to directly compare cross sections measured in the two experiments. As indicated in Section II., we can compare our data with the simple functional dependence on x and s predicted by triple Regge theory. The high cross section of the inclusive process assures that we will have an adequate data sample for these comparisions, in contrast to the study of exclusive processes.

We expect to detect the $\overline{K^0}$ by the decay $K_S^0 \rightarrow \pi^- + \pi^+$ We are very familiar with the properties of pair spectrometers through our work on K_S regeneration in E-82, and thus expect no problems in this area.

II. INCLUSIVE REACTIONS AND TRIPLE REGGE THEORY

Simple Regge pole exchange applied to exclusive pion charge exchange, K_S regeneration in carbon and particle antiparticle differences of total cross sections has proved to be remarkably sucessful at Fermilab energies. Since all of these processes vanish as s becomes large, one turns to inclusive reactions for the study of strong interaction dynamics.

For the general inclusive process

$$A + B \to C + X \qquad p_1 + p_2 \to p_3 + p_4 \qquad (3)$$

we can use the variables

$$s = (p_1 + p_2)^2 \qquad t = (p_1 - p_3)^2 \qquad M^2 = p_4^2 = (p_1 + p_2 - p_3)^2 = t + m_2^2 + 2m_2(E_1 - E_3)$$

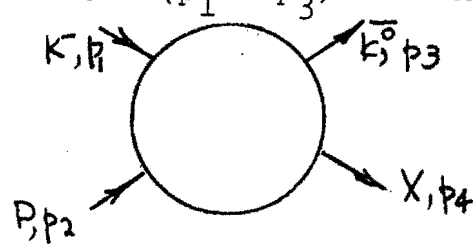

For large s and small t, useful relations are

$$s = 2m_2E_1 \qquad x = E_3/E_1 \qquad M^2 = t + m_2^2 + s(1 - x)$$

The triple Regge description of inclusive processes is arrived at by first using t channel Regge poles to describe (3) for arbitrary M^2. This requires $s \gg M^2$ or $(1 - x) \ll 1$ One can then use the Mueller generalized optical theorem [1] to express the total inclusive cross section as the absorptive part of the three body forward amplitude $A + B + \bar{C} \to A + B + \bar{C}$ This amplitude is in part describe by a Reggeon-proton forward scattering amplitude which can itself be described by a Regge exchange if $M^2 \gg 1$. We include a graphical description of thes steps as Fig.1., taken from an article by Field and Fox [4]. A more formal description was first given by de Tar et al.[6].

The result of this series of Reggeizations can be written as follows [2]

$$d^2\sigma/dtdx = (1/16\pi)\sum_{ijk} B_i(t)\, B_j(t)\, (s/M^2)^{\alpha_i(t) + \alpha_j(t) - 1}$$

$$\cdot \left[- \frac{1 + \tau_i e^{-i\pi\alpha_i(t)}}{\sin(\pi\alpha_i(t))} \right] \left[- \frac{1 + \tau_j e^{i\pi\alpha_j(t)}}{\sin(\pi\alpha_j(t)} \right] B_{ijk}(t)\, M^{2\alpha_k(0)-2} .$$

where i,j,k are all allowed Regge/Pomeron trajectories, $B_i(t)$ is the Regge $K^-K^oR_i$ residue function,

$$-(1 + \tau_i e^{-i\pi\alpha_i(t)})/\sin(\pi\alpha_i(t))$$

is the signature factor, and $B_{ijk}(t)$ is the triple Regge vertex function. If i,j,k are all Reggeons, the dependence on s,x is

$$d^2\sigma/dtdx = s^{-\frac{1}{2}}\, (1 - x)^{-\frac{1}{2}-2t} \qquad (5)$$

If k is the Pomeron

$$d^2\sigma/dtdx = (1 - x)^{-2t} \qquad (6)$$

where we assume $\alpha_i(t) = \frac{1}{2} + t$ for all Regge trajectories, and $\alpha(0) = 1$ for the Pomeron.

An analysis of (PP) $\Rightarrow$ (PX) using all available data has been carried out by Field and Fox [4] using triple Regge theory. While the fits to data are excellent, the authors note that the large number of pole terms possible and the neglect of interferenece terms ($i \neq j$) makes it difficult to assess the importance of individual poles and to test for violation of the theory.

Fox has analysed preliminary inclusive data for

$$\pi^- + P \rightarrow (\pi^o, \eta) + \text{neutrals}$$

using a modification of the above theory [5]. The reactions fitted invole only ρ and A_2 respectively, and show a dependence on x given by (6).

Within the triple Regge region, the inclusive kaon $d^2\sigma/dxdt$ should be given by a linear combination of (5) and (6) with coefficients depending on t. Three Regge graphs involving ρ and A_2 give (5), Reggeon-Reggeon-Pomeron graphs give (6). Some possibilities for the analysis are as follows

1.) A study of the dependence on s for fixed x,t will identify the Pomeron and non-Pomeron contribution to the cross section. One expects

$$d^2\sigma/dxdt = A_P + A_{nP}\, s^{-\frac{1}{2}}$$

2.) Zeroes of the signature factor (WSNZ) are known to be associated with dips in $d\sigma/dt$ for exclusive pion charge exchange. While dips should not occurr here (all signature factors are not zero at the same time), the zero in all ρ exchange terms at $t = -0.55$ should allow a direct comparision of $(K^-P) \rightarrow (\overline{K}^0)$ and $(\pi^-P) \rightarrow (\eta)$ All of the A_2 terms should vanish at $t = -1.65$, allowing direct comparision with $(\pi^-P) \rightarrow (\pi^0)$.

3.) The triple Regge vertices in K^-P charge exchange include all π^-P charge exchange vertices plus ρ-A_2 interference terms. A comparision of $d^2\sigma/dxdt$ for the two experiments using SU_3 and factorization could be used to determine the interference terms. They would be absent if $\alpha(t)$ is the same for ρ and A_2; in any case, the $s^{-\frac{1}{2}}$ dependence should make them small at high energies.

III. EXPERIMENT - INTRODUCTORY REMARKS

In this experiment we study those (K^-P) interactions which produce K_S^0 at angles between 0 and approx. 35 mrad. to the incident beam direction.

The experiment will be set up in the charge M4 beam proposed by C.Brown and L.Read. We thank the authors for providing us with a preliminary draft of their technical memorandum which we include as Appendix 1.

The setup consists of a small hydrogen target and a "long lived neutral Vee" spectrometer.

The charged particles (incident kaons and locally produced secondaries) which emerge from the target are swept out of the sensitive aperture of the detector by a post-target magnet. This allows us to detect non interacting kaons without biasing the inclusive nature of the experiment.

The detector ("long lived neutral Vee spectrometer") consists of the standard arangement of wire chambers and counters which bracket an analysing magnet (in this case the M4B8). Together with our collaborators we have installed and sucessfully operated such a spectrometer in the kaon regeneration experiment 82.We will investigate the possibility of using that spectrometer for this experiment.

The important variables in this experiment are s,t,x (see page 3). The details of the apparatus most closely relato each of them are:

- s Momentum of the incident beam
- t Angle between the beam and the axis of the detector.
- x Length of the drift space.

We will collect our data in a series of runs for which these variables are adjusted to cover the region of interest to the

physics of the experiment.

In the following pages, some of the technical aspects of the experiment are discussed in more detail.

IV. EXPERIMENT - TECHNICAL DETAILS

BEAM

We propose to use the beam as described in the technical memorandum of Appendix 1., with the following modifications. The Cerenkov counter is moved from the 1300 ft. enclosure to the berm pipe between the 1300 ft. enclosure and the MX4 pit (perhaps part of the berm pipe itself could be used as the Cerenkov counter). The last two quadrupoles are moved from the MX4 pit to the 1300 ft. enclosure. We propose, as part of this experiment, to implement the charged M4 beam and its momentum tagging system, which would become a permanent laboratory installation.

TARGET

The rate estimates are given for a 0.3 m. liquid hydrogen target. Such a target would produce 1% secondary interactions for the outgoing neutral kaons. We hope to use one of the several targets built for the now completed experiments.

The t-aperture of the detector varies from

$$\Delta t \simeq 1.3\ (\mathrm{GeV/c})^2 \text{ at } P_K = 150\ \mathrm{GeV/c}$$

to

$$\Delta t \simeq 0.7\ (\mathrm{Gev/c})^2 \text{ at } P_K = 50\ \mathrm{GeV/c}$$

To gain access to high values of -t we intend to have the beam traverse the target at an angle (typically 15 to 35 mrad). To eliminate problems in pattern recognition due to extra tracks we will sweep the incident (non interacted) beam and the charged interaction products out of the detection apparatus. To achieve this we propose to bracket the target with two magnets. In the high -t configuration the incident beam will be deflected slightly by the beam transport system, to have it traverse the target at its intersection with the axis of the apparatus.

The beam will be focussed on a small veto counter, well downstream of the target. This minimizes the chance that the veto counter be hit by a secondary particle from the target.

DETECTION EQUIPMENT AND TRIGGER

The detection equipment (Fig.2.) is a wire chamber spectrometer like the one used in the kaon regeneration experiment 82. Downstream of the target there is a vacuum drift space, whose length is adjusted to maximize the detection efficiency and minimize the incident beam interference, both as a function of the incident beam momentum.

Then follows a standard wire chamber spectrometer with two 10 m. legs bracketing the M4B8 analysing magnet.

The sweeping magnet discussed previously will eliminate from the detector all charged particles produced at the target.

An interacting incident K^- is indicated (beam trigger) by a coincidence of the Cerenkov counter with a beam telescope, in anticoincidence with the previously mentioned veto counter.

The event trigger is a coincidence of a beam trigger with a set of signals which indicate the presence of at least one particle upstream of the analysing magnet and the presence of two particles at the downstream end of the apparatus. The expected absence of long lived neutral Vees, other than K^o and Λ makes a more complicated triggering scheme (such as the one used in experiment 82) unnecessary.

SOURCES OF BACKGROUND.

We consider the following sources of background triggers:

Charged secondaries from kaon initiated interactions

Long lived neutral Vees produced by pions.

Unwanted long lived neutral Vees produced by kaons

The number of triggers produced by charged secondaries from the target(which are not swept out of the system by the post-target magnet) is hard to estimate. We guess that with a post-target magnet of p_T = 0.9 GeV/c approximately 1/1000 of all interactions will yield a false trigger due to insufficient sweeping. The total inelastic cross section for (K^-P) interactions is approx. 20 mbarn, the cross section for $(K^-P) = (K^o_S X)$ is approx. 0.2 mbarn, while triggering efficiency is approx. 50%. This leads to an estimate of approx. 25% in this class.

The Cerenkov counter will occasionally mislabel a pion as a kaon. For pion/kaon flux ratios of eight (Appendix 1.) this is not a problem at the trigger level, but requires reasonable corrections in the final results. Monitoring runs with incident pions will provide the information necessary to make these corrections. Indeed these monitoring runs will yield the preliminary information to elvaluate the parameters for the study of pion initiated interactions of the type mentioned in Appendix 2.

The "unwanted" long lived neutral Vees in the study of $(K^-P) = (K^oX)$ are kaons outside the triple Regge region and lambdas produced directly or by the decay of directly produced neutral sigmas. The detection efficiency of the proposed apparatus falls off quickly when x decreases. This is due to the fact that the drift space is "tailored" to the incident beam energy.Low energy kaons decay upstream and their decay pions spread too much to be detected. On the other hand it is the goal of this experiment to investigate the extent of the triple Regge region . A preliminary analysis of initial data may well cause us to run for some time with a bias towards low values of x (high momentum beam with low momentum drift space).

While $(K^-P) = (\Lambda X)$ is again a reaction of interest, its contribution to background triggers will be small, since interactions at $x > 0$ dominate.

In conclusion, background triggers from interactions in the target seem to be of manageable proportions. We have not considered here the possible triggering difficulties due to troubles with the beam optics. These do not appear to have been serious in other beam lines.

RATE ESTIMATES

We base our estimate of the cross section for the reaction $(K^-P) \Rightarrow (K^o_S X)$ on the measurements of $(K^-P) \Rightarrow (K^o_S X)$ at low energies[7] and of $(\pi^-P) \Rightarrow (\pi^o X^o)$ at high energies (5) This yields

at $t = 0$ $\quad \int_{0.8}^{1.0} dx\, d^2\sigma/dxdt = 0.2 \cdot 10^{-27}\ cm^2/(GeV/c)^2$

and $\quad \int_{2.0}^{3.0} dt \int_{0.8}^{1.0} d^2\sigma/dxdt = 3 \cdot 10^{-30}\ cm^2$

Assuming the charged kaon fluxes of Appendix 1., a 0.3 m. liquid hydrogen target and computed detection efficiencies, we estimate the following data collection rates (events/hour)

P_K(GeV/c)	$0 < -t < 1$	$2 < -t < 3$
50	4000	33
100	2000	17
150	400	4

Since we have not found any large sources of background triggers, no consideration has been given to equipment dead time effects.

V. EXPERIMENTAL EQUIPMENT

Our current thoughts call for the following sources of the experimental equipment.

The installation of the charged M4 beam (including the permanent tagging equipment) will be a meson laboratory facility It will be implemented by the experimenters in collaboration with the Meson Laboratory staff. Its cost will be borne by Fermilab. The configuration will be as discussed in Appendix 1. and in this proposal, except for modifications to be discussed between the Meson Lab and the experimenters.

The small liquid hydrogen target would be constructed by Fermilab, following specifications by the experimenters.

The MX4 pit with the M4B7 and M4B8 magnets and its power supplies will be used. The second target magnet is available but its loan has not yet been requested.

The responsibility for the detection equipment (counters, wire chambers, wire chamber readout system, cables, etc.) would be with the experimenter. A large portion of this equipment might be obtainable on a loan basisfrom other experimenters, thus reducing the cost and lead time.

Standard experimental services, such as PREP equipment and beam line control equipment, would be available to the experimenters.

VI. PERSONNEL AND RESEARCH SUPPORT.

Our present staff of two senior PhD level physicists and one graduate student is clearly insufficient to carry out the proposed experiment, as is our present level of grant support. It is our intent to augment the UCSD group, to include Fermilab collaborators and at least one outside collaborator.

We have been advised by the National Science Foundation that an increase in the support level is possible but contingent upon our being principal investigators for an approved experiment.

If the proposal were approved, we would then expect to acquire the funding and manpower appropriate to the experiment, before the signing of an agreement.

REFERENCES

(1) Mueller,A.h., Phys.Rev. D2 2963 (1970)

(2) Horn and Zachariasen, "Hadron Physics at Very High Eneregies", Benjamin (1973) Most of the relevant theory is discussed in chapter 6, with appropriate original references.

(3) See for example: G.C.Fox, AIP Conference Proceedings 15 (High Energy Collisions, 1973), C.Quigg, Editor (1973)

(4) R.D.Field and G.C.Fox, "Triple Regge and FMSR Analysis of the Inclusive Reaction PP=PX" Nuc.Phys. B80, 367 (1974)

(5) G.C,Fox and D.J.Mellema, Addendum fo Fermilab Proposal 350 We thank G.C.Fox for his advice and many helpful comments.

(6) C.E.de Tar et al., Phys.Rev.Lett. 26, 675 (1971)

(7) J.V.Beaupre et al., Nuc.Phys.B30, 381, (1971)

APPENDIX 1

Fermilab

TWO ADDITIONAL CHARGED BEAMS IN THE MESON AREA

C. N. Brown and A. L. Read
February, 1975

We propose two new charged beams in the Meson Area. The present M4 neutral kaon beam can be interchangeably converted into a broad band charged beam with momentum capabilities up to 200 GeV/c. At 100 GeV/c this beam would contain a very favorable flux of at least 10^5 antiprotons per pulse. A simple version of the M5 test beam is also proposed which would transmit 5×10^5 π^-/pulse at 30 GeV/c or 1×10^5 π^-/pulse at 60 GeV/c. The implementation of both of these designs is quite inexpensive and involves EPB dipoles and quads currently on hand.

A. A Charged M4 Beam

This proposal for the conversion of the M4 7.25 milliradian neutral beam in the Meson Area into a charged beam has been largely motivated by two factors:

i) the relative dearth of new proposals for experiments to utilize the existing M4 neutral beam;

ii) the extremely large number of proposals for Meson Area experiments which require a beam of charged hadrons.

We describe below the design details of a proposed conversion of the M4 beam into a charged particle ($\pi^{\pm}$, $K^{\pm}$, p and $\bar{p}$) beam. The beam would have a maximum momentum of 200 GeV/c. A relatively modest rigging effort (~1 shift) would enable the conversion of the new charged beam back into the existing M4 neutral beam configuration, and vice versa. The charged beam would contain a parallel section to enable the possible use of a "Kycia" type differential Cerenkov counter for particle identification.

The conversion of the M4 beam to a charged beam within the confines of the 14" berm pipe involves alternate left and right bends causing the charged line to zig-zag within a few inches of the present neutral kaon line. This design leads to a very small dispersion and, hence, the possibility of a large momentum bite and concomitant substantial article flux.

Table I lists the current M4 beam elements in the various M4 beam enclosures and the projected charged beam elements. Figure 1 indicates a first order beam envelope as calculated by TRANSPORT. The optics is a simple two-stage system in both planes with a parallel section in the second section. A second order TRANSPORT run indicates that the final beam spot will be less than 1 cm

diameter even with a 10% FWHM $\Delta p/p$ momentum bite. The minimum momentum bite will be 2% FWHM.

The offset in the collimators required at the 400', 600', and 1000' gallerys can be affected either by physical movement of the present neutral beam collimators or by addition of inserts to the collimators, thereby shifting their effective center. There are no other geometrical changes required to change from the neutral to the charged configuration; thus the changeover would require less than one shift. A power supply change might also be required to ensure stability at the very low currents needed in the sweeping magnets.

Estimates of the M4 charged beam intensities can be made based on extrapolations of particle production data at 3.5 mrad by Experiment 104 and at 7.25 mrad by Experiment 82. Estimates of $\bar{p}/\pi^-$ intensity ratios are based on a discussion of $\bar{p}/\pi^-$ ratios in Proposal-302.

Proton beam energy assumed:	300 GeV
Proton beam intensity assumed:	10^{13} protons/pulse
Proton beam target assumed:	8" long Be target
$\Delta p/p$ acceptance - defined by momentum slit M4C3:	±5% HWHM
$\Delta p/p$ resolution limit (by using minimal p/p acceptance):	±1% HWHM
$\Delta p/p$ acceptance amount in M4C beam intensity estimates:	±5%
Beam diameter (2nd order transport run ±5% $\Delta p/p$):	1.2 cm x .6 cm

Momentum	Particle	Intensity Per Pulse	
	$\pi^{\pm}$	K^{+} (*)	$\bar{p}$
50	10^7	2×10^6	2×10^5
100	2×10^6	5×10^5	10^5
150	5×10^5	10^5	

A crude check of the charged particle yield was made by us in the M4 beam using a simple scintillator telescope off-center at the 600' enclosure. These measurements confirmed the predictions to within a factor of about 3. Note: with the $\pi^-/\bar{p}$ ratio indicated at 100 GeV/c, it should be possible with MWPC's and a differential Cerenkov counter in the incident beam to tag and determine the momentum very accurately for at least 10^5 $\bar{p}$/pulse. It is possible that the Preuss counter currently in the M1E branch would be available and could be used for particle identification.

The main expense in implementing this proposed beam involves the assignment of four 3Q60 quads, two 2Q120 quads, and the one 5 ft EPB dipole to be exchanged for a 10' EPB dipole.

B. The M5 Test Beam

We attempt here to revive a previous, very simple design for the M5 charged particle test beam. The motivations for the design at this time include two factors.

(*) K^- fluxes are expected to be lower then K^+ fluxes by a factor 1.5 - 2 (personal communication by L. Read)

i) The lack of a reasonably intense, simple-to-operate beam facility at Fermilab.

ii) The large number of short tests and quick experiments which the Meson Laboratory has inadequately attempted to accommodate in the three charged beams in the last year.

The envisioned configuration of this beam is a simple two-stage point-to-point focussing system. The optics should enable the beam to run either with a high flux and rather poor spot or a smaller flux with a much improved focus. The focus is kept well upstream in the M5 enclosure so that adequate space exists for both test facilities and a beam stop before the beam reaches the Meson Detector Building floor.

Table II lists the proposed elements in the beam line. Figure 2 indicates a first order beam envelope as calculated by TRANSPORT. A second order calculation reveals a beam spot size of about .2 cm diameter for .1% FWHM $\Delta p/p$, the minimum momentum bite, and a 1 cm diameter spot for .6% FWHM $\Delta p/p$, the maximum momentum bite. We feel this is adequate for such a test beam.

Flux estimates for this beam have been made using the

Sanford-Wang fit as modified by Wang to fit the data of Baker, et al, in the M1 beam. The pion yield is calculated for 3×10^{12} 400 GeV protons incident on an 8" Be target per pulse and a .5% FWHM $\Delta p/p$ momentum bite.

Pion Flux Per Pulse

	π^+	π^-
20 GeV/c	8×10^5	6×10^5
40 GeV/c	5×10^5	4.5×10^5
60 GeV/c	1.5×10^5	1.5×10^5

This beam could be built in either a 30 GeV/c maximum momentum version or a 60 GeV/c maximum momentum version depending on the availability of EPB dipoles. 30 GeV/c requires four 3Q60 EPB quads, three 5-1.5-120 EPB dipoles, and one 5-1.5-60 EPB dipole. Upgrading to 60 GeV/c requires an additional three 5-1.5-120 EPB dipoles. One pair of x, y collimators will suffice to define both the momentum and angle aperature of the beam line.

Currently some power supplies, control rack space and buss-work in the M5 tunnel exist having been installed during the original construction phase of the Meson Laboratory. Besides the magnets, about 1000 feet of 4" beam pipe will be required for the installation of the beam.

TABLE 1

M4 Beam Line Elements

	Z (ft)	Description
Front End Hall	246	Present beam stop, replace with 3Q60
	254	Present 5-1.5-120 dipole, replace with 5-1.5-60 dipole
	262	Add 3Q60
400' Enclosure	368	Fixed collimator (½" x ½"), must be 2" x 1" for max. charged beam
	390	Muon spoilers presently not used, replace with beam stop
600' Enclosure	655	Horizontal collimator, charged beam centered 7 cm east
	661	Vertical collimator, first focus for charged beam
	667	5-1.5-120 sweeping magnets
1000' Enclosure	1008	Add 3Q60 quadrupole
	1018	Add 3Q60 quadrupole
	1021	Horizontal collimator, charged beam centered 7 cm west
	1027	Vertical collimator
	1040	5-1.5-120 sweeping magnets
1300' Enclosure	1322	Possible location of differential Cerenkov counter
	1350	Add 5-1.5-60 EPB dipole
1600' Experimental Pit	1605	Add 3Q120 EPB quadrupole
	1616	Add 3Q120 EPB quadrupole
	1710	Second focus of charged beam

Figure 1

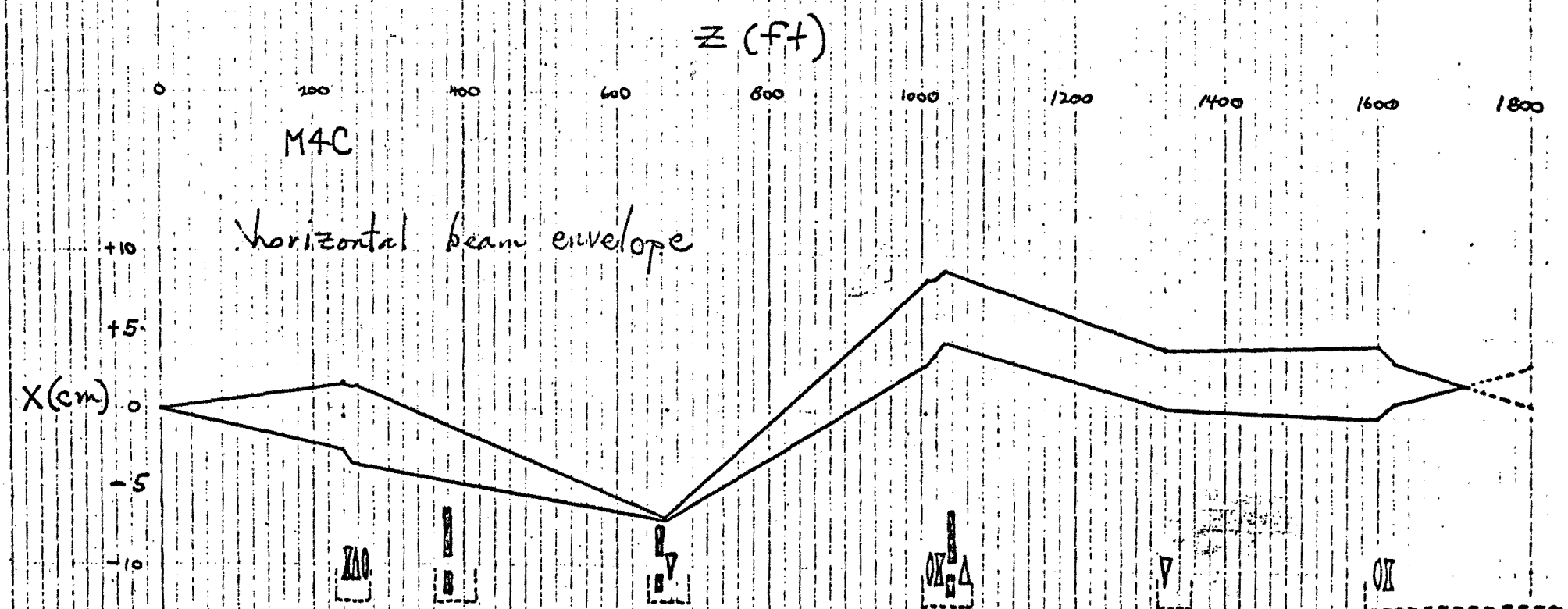

Schematic of M4 enclosures

TABLE 2

M5 Test Beam Elements

	Z(ft)	Description
Front End Hall	62.0	Vertically focussing 3Q60 quadrupole
	68.5	Horizontally focussing 3Q60 quadrupole
	126.0	5-1.5-120 EPB dipole
	135.0	5-1.5-60 EPB dipole
	144.0	5-1.5-120 EPB dipole (for 60 GeV/c)
M5 Tunnel	685.0	Horizontal collimator
	690.0	Vertical collimator, first focus
	701.75	5-1.5-120 EPB dipole (for 60 GeV/c)
	713.25	5-1.5-120 EPB dipole
	724.75	5-1.5-120 EPB dipole
	736.25	5-1.5-120 EPB dipole
M5 Enclosure	1178.5	Horizontally focussing 3Q60 quadrupole
	1185.0	Vertically focussing 3Q60 quadrupole
	1250.0	Second focus

Figure 2

Beam envelope for minimum momentum bite

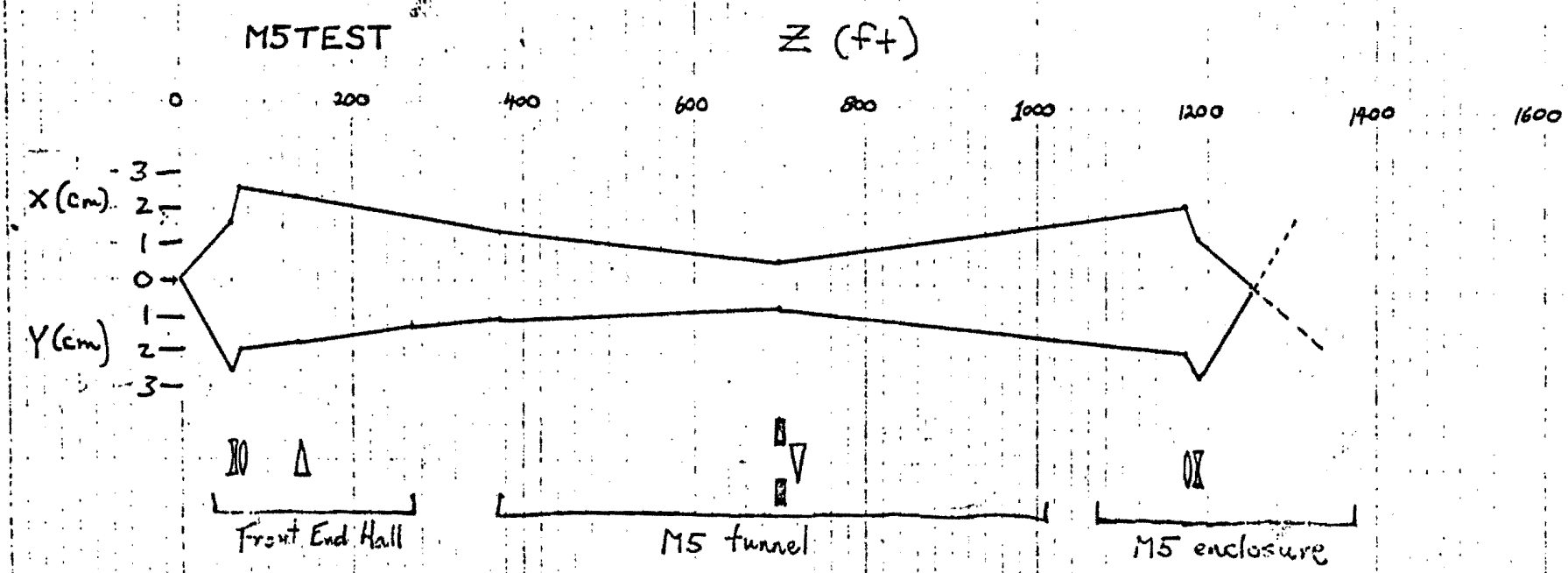

Appendix 2

The following reactions are potential candidates for inclusive studies using a K^s spectrometer and hydrogen target.

Projectile	Detected Particle	Exchanged Particle
π^+, π^-	K^o	K^*, K^{**}
K^+, K^-	$K^o, \overline{K^o}$	A_2, ρ
$\overline{P}$	$\overline{\Lambda}$	K, K^*, K^{**}, Q

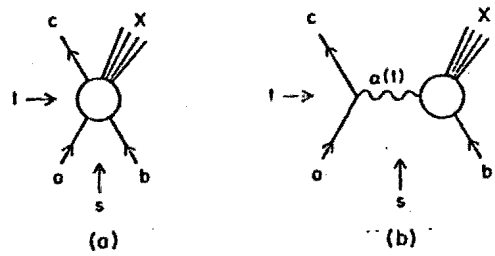

Fig. 1. (a) Shows the inclusive process $ab \to cX$, where a, b, and c are definite particles and X represents anything. (b) Shows the exchange of a Regge-pole $\alpha(t)$ in the t-channel for the inclusive process $ab \to cX$.

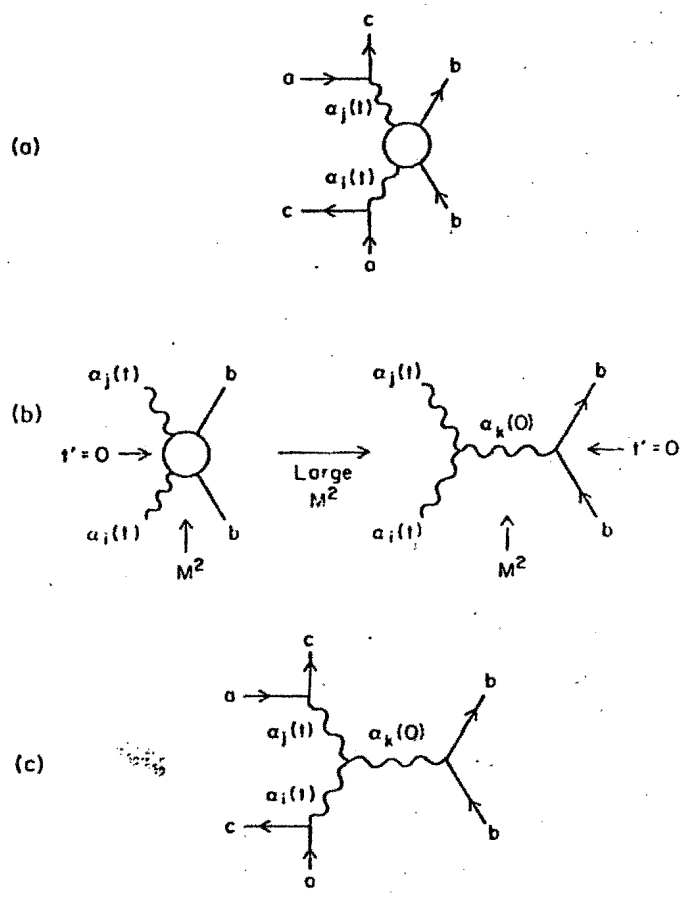

Fig. 2. (a) Diagram which corresponds to squaring and summing over all states X in fig. 1b. (b) Reggeon-particle forward scattering which at large M^2 is assumed to be dominated by the exchange of a Regge pole $\alpha_k(0)$. (c) Diagram corresponding to the triple-Regge region for the inclusive process $ab \to cX$.

FIGURE 1

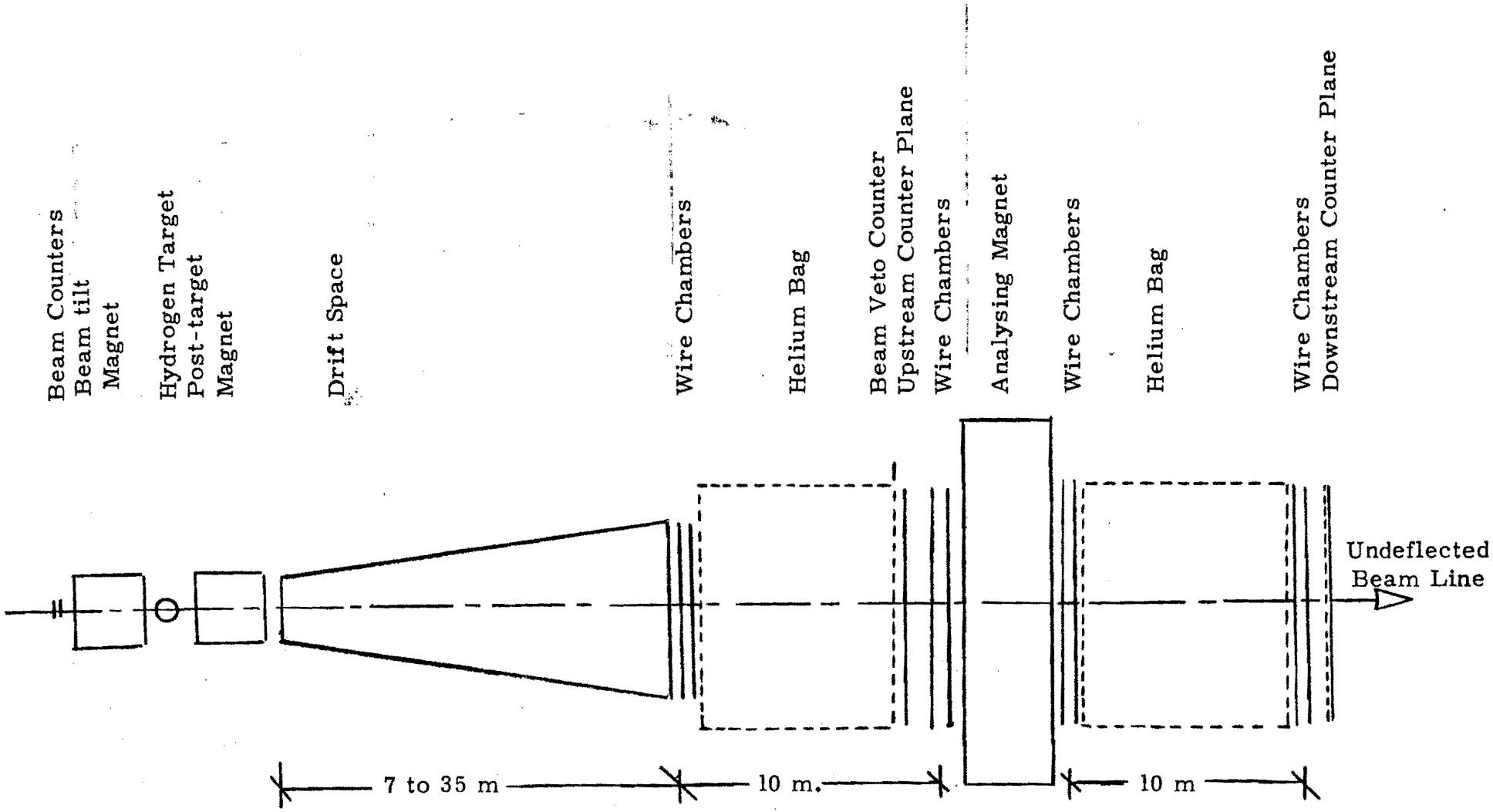

K⁻ CHARGE EXCHANGE INCLUSIVE

Schematic Equipment Layout

20 February 1975

Figure 2.

obtained using the $\bar{K}^0\pi^-\Delta^+$ fitted parameters. In addition to the vector $K^*(892)$, the model has a scalar $K\pi$ resonance at 1080 MeV with a width of 240 MeV. It should be realized that if $\mathrm{Re}\,\rho_{ll}$ are equal to zero, the daughter resonances in this model have the same masses as the parents. Thus it is the fact that $\mathrm{Re}\,\rho_{0\frac{1}{2}} = 0.78$ that causes the scalar K^* to be at 1080 instead of 892 MeV. Furthermore, it is the low mass tail of this K^* and the isospin 1/2 non-resonant S-wave, interfering with the $K^*(892)$ P-wave which causes the observed $\bar{K}^0\pi^-$ decay asymmetry.

In summary, we have presented positive evidence for the existence of a $\bar{K}^0\pi^-$ decay asymmetry in reactions (1) and (2) at 3.3 GeV/c momentum. The effect is quite similar in both reactions. An attempt was made to describe the asymmetry using the Lovelace-Veneziano model and qualitative agreement was found.

It is a pleasure to acknowledge the hospitality of the Oxford Bubble Chamber Group during an extended visit by the author. The scanning and measuring teams at both UCLA and Oxford are to be thanked for their efficient contributions to this study.

REFERENCES

[1] T.G. Trippe, C.-Y. Chien, E. Malamud, J. Mellema, P.E. Schlein, W.E. Slater, D.H. Stork and H.K. Ticho, Phys. Letters 28B (1968) 203.
[2] C. Fu, A. Firestone, G. Goldhaber and G.H. Trilling, Nucl. Phys. B18 (1970) 93.
[3] P.E. Schlein, UCLA preprint 1040 (1969); Invited paper at the Argonne Conf. on $\pi\pi$ and πK interactions.
[4] CERN-Bruxelles-Munchen Collaboration, Nucl. Phys. B16 (1970) 125.
[5] J. Goldberg, E. Huffer, M. Laloum, G. Lamidez, A. Rougé, B. Haber, G. Yekutieli, A. Rossi, P. Serra, G. Bakker, W. Hoogland, R. Barloutaud and J. Scheuer, Phys. Letters 30B (1969) 434.
[6] D.D. Carmony, R.L. Eisner, A.C. Ammann, A.F. Garfinkel, L. Gutay, D.H. Miller, L.K. Rangan and W.L. Yen, Phys. Rev. D2 (1970) 30.
[7] P.A. Schreiner, D.H. Stork, A. Clark, D. Saxon and L. Lyons, Nucl. Phys. B24 (1970) 157.
[8] E. Colton, S. Prum, P. Schlein and A.J. Verglas, Nucl. Phys. B17 (1970) 117.
[9] C. Lovelace, CERN preprint TH1041 (1969); Invited paper at the Argonne Conf. on $\pi\pi$ and πK interactions.

B.8 Nuclear Physics B30 (1971) 381-397. North-Holland Publishing Company

EXPERIMENTAL CHARACTERISTICS OF THE CHARGE-EXCHANGE K^0 PRODUCING REACTIONS IN K^+p AND K^-p INTERACTIONS

Aachen-Berlin-CERN-London-Vienna and Bruxelles-CERN Collaborations

J.V. BEAUPRE, M. DEUTSCHMANN, H. GRÄSSLER and P. SCHMITZ
III. Physikalisches Institut der Technischen Hochschule, Aachen

U. GENSCH, W.D. NOWAK, H.J. SCHREIBER and M. WALTER
Institut für Hochenergiephysik der Deutschen Akademie der Wissenschaften zu Berlin, Zeuthen

E. DE WOLF, F. GRARD *, P. HERQUET, L. PAPE, P. PEETERS, F. VERBEURE and R. WINDMOLDERS *
Laboratoire Interuniversitaire Belge des Hautes Energies, Bruxelles

A. ANGELOPOULOS **, P.V. CHLIAPNICOV ***, V.T. COCCONI, O. CZYZEWSKI +, D. DRIJARD, P. DUINKER, W. DUNWOODIE, A. ESKREYS ++, Y. GOLDSCHMIDT-CLERMONT, A. GRANT, J.D. HANSEN +++, V.P. HENRI, W. KITTEL, D. LINGLIN ‡, S. MATSUMOTO ‡‡, J. MEYER, D.R.O. MORRISON, F. MULLER, S. NIELSEN, Z. SEKERA and R. STROYNOWSKI
CERN, European Organisation for Nuclear Research, Geneva

P.J. DORNAN, G.A. GRAMMATIKAKIS, B.R. KUMAR and A. MUTALIB
Physics Department, Imperial College, London

B. BUSCHBECK, A. FROEHLICH, P. PORTH and H. WAHL ‡‡‡
Institut für Hochenergiephysik der Österreichischen Akademie der Wissenschaften, Vienna

Received 13 April 1971

* Also at Faculté des Sciences, Centre Universitaire de l'Etat, Mons.
** Now at the University of Athens.
*** Visiting Scientist from the Institute of High Energy Physics, Serpukhov.
+ Visiting Scientist from the Institute of Nuclear Physics, Cracow.
++ Now at the Institute of Nuclear Physics, Cracow.
+++ Now at the University of Illinois, Urbana, Illinois.
‡ Now at the Laboratoire de Physique, Ecole Polytechnique, Paris.
‡‡ Visiting Scientist from Chuo University, Tokyo.

Abstract: A study is made of the charge-exchange reactions $K^+p \to K^0X^{++}$ at 5 and 8.2 GeV/c and $K^-p \to \bar{K}^0X^0$ at 10.1 GeV/c, where X denotes the system of all secondary particles different from K^0, with effective mass M. In general it is found that the production properties of the K^0 and of the X system are similar for incident K^+ and K^- mesons. The cross section for K^0 production is ≈ 40% of the total inelastic Kp cross section in all cases studied. The mass spectrum of X, $d\sigma/dM$, outside the resonance region, increases exponentially with M, while the $d\sigma/dt'$ distributions decrease exponentially as $\exp(-At')$ for $0 < t' < 1.0$ GeV^2, with the value of A depending on the mass M as $M^{-\alpha}$ ($\alpha \approx 2$). The scaling effect predicted by Feynman is observed for the distributions of $x = p^*_L/p^*_{L\,max}$ in the K^+p reactions at 5 and 8.2 GeV/c. It is shown that a simple two-dimensional parametrisation in terms of M and t' can describe satisfactorily most of the experimental results.

1. INTRODUCTION

In this paper we present results of a study of the reactions

$$K^+p \to K^0_{seen}X^{++}, \quad (1)$$

$$K^-p \to \bar{K}^0_{seen}X^0, \quad (2)$$

produced by 5 and 8.2 GeV/c positive and 10.1 GeV/c negative kaons, interacting in the 150 cm British and 80 cm and 200 cm CERN hydrogen bubble chambers. The symbol X indicates the system of all secondary particles other than K^0. The experimental results on K^0 production in reactions (1) and (2) are presented in sect. 2, where we also derive simple empirical formulae to describe the mass M and four-momentum-transfer t' distributions. In sect. 3 a simple overall parametrisation of the data is presented and discussed.

Neutral kaons are particles especially well-suited for this type of study since they are identified easily and observed with little bias, independent of their momentum and emission angle. Experiments of this type, often called "inclusive" [1], are to a large extent complementary to the exclusive ones, which study definite final states. An inclusive bubble chamber investigation is equivalent to a single-arm counter experiment, but has the advantage of covering the full solid angle of particle emission and of studying the contributions to the various effects observed, deriving from final states of different multiplicities.

In general the data on the production characteristics of a secondary particle can be presented fully in terms of only two variables. Although several pairs of variables, in principle equivalent, can be used, some choices are more suitable than others for a specific purpose. In this paper we present the data on K^0 production in the form of double-differential cross sections using several pairs of variables, such as: (a) laboratory momentum p_{lab} and laboratory angle θ_{lab} of the K^0 mesons; (b) effective mass M of all produced particles other than K^0 and squared four-momentum transfer (t or $t' = |t - t_{min}|$) from incoming to outgoing kaon; and (c) normalised longitudinal

The data used for this work consist of 6 535 events at 5 GeV/c and 10 479 events at 8.2 GeV/c of K^+p interactions and of 18 228 events of K^-p interactions at 10.1 GeV/c, each event containing a K^0 observed to decay into two charged pions. The corresponding μb equivalents are 0.29, 0.173 and 0.138 μb/events, at 5, 8.2 and 10.1 GeV/c, respectively.

2. EXPERIMENTAL RESULTS

2.1. *Cross sections*

The total number of events in which a K^0 is seen to decay into two charged pions, the total cross section for K^0 production and the partial cross section for channels of different charged multiplicities are listed in table 1 for the three experiments considered. All K^0 cross sections are corrected for decays outside the visible region of the chamber and for unseen decay modes. They are obtained by normalising the total number of events found on a part of the available films (corrected for scanning losses) to the values [2] of the total Kp cross sections listed in the first row of the table. The values of the inelastic part of the Kp cross sections are also listed.

As can be seen, the fraction of the inelastic cross section associated with K^0 production $\sigma_{K^0}/\sigma_{inel}$ is close to 40% for both K^+ and K^- reactions at the incident momenta studied. This is essentially true also for results of other experiments at 3 and 3.5 GeV/c (see fig. 1). It is interesting to note that a ratio of about 40% is found in the K^-p experiment at 10.1 GeV/c also for the ratio σ_n/σ_{inel}, which corresponds to the other possible charge exchange reaction, $K^-p \to nX^0$.

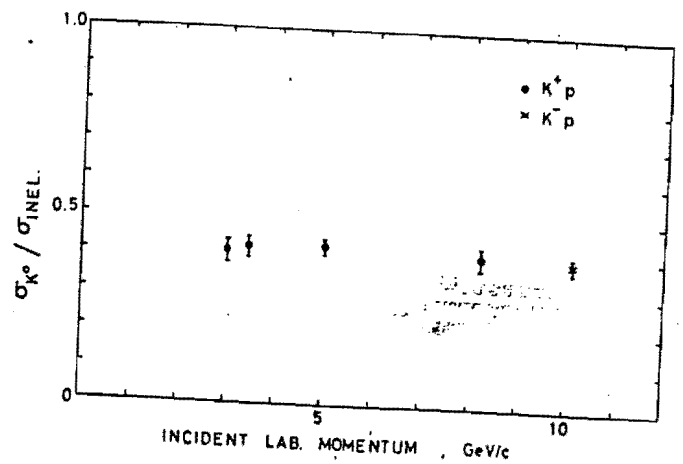

Fig. 1. Ratio of K^0 production cross section to total inelastic cross section as

Table 1
Total and partial K^0 cross sections, and number of events for the reactions (1) and (2). All K^0 cross sections are corrected for unseen K^0 decay modes and for decays outside the chamber.

Reaction		K^+p at 5 GeV/c	K^+p at 8.2 GeV/c	K^-p at 10.1 GeV/c
σ_{tot} (Kp)		17.2 ± 0.2 mb	17.2 ± 0.1 mb	22.5 ± 0.2 mb
σ_{inel} (Kp)		13.6 ± 0.3 mb	13.8 ± 0.3 mb	19.4 ± 0.2 mb
total number of events with K^0_{seen}		6535	10479	18228
total cross section for K^0 prod., σ_{K^0}		5.76 ± 0.21 mb	5.76 ± 0.33 mb	7.58 ± 0.18 mb
0-prongs	number of events with K^0_{seen}			1230
	σ			0.60 ± 0.06 mb
2-prongs	number of events with K^0_{seen}	5133	6027	9453
	σ	4.24 ± 0.20 mb	3.09 ± 0.21 mb	3.66 ± 0.24 mb
4-prongs	number of events with K^0_{seen}	1386	3889	6703
	σ	1.48 ± 0.12 mb	2.40 ± 0.15 mb	2.79 ± 0.18 mb
6-prongs	number of events with K^0_{seen}	16	560	818
	σ	0.04 ± 0.01 mb	0.27 ± 0.05 mb	0.50 ± 0.04 mb
8-prongs	number of events with K^0_{seen}		3	24
	σ		0.002 ± 0.001 mb	0.03 ± 0.01 mb

2.2. *Differential-cross-section distributions*

In fig. 2 we present the $d^2\sigma/dp_{lab}\,d\Omega_{lab}$ distributions, as functions of p_{lab}, for various intervals of the emission angle θ_{lab}. The events were weighted by the factor $(2\pi \sin\theta_{lab})^{-1}$, which takes into account the summation over relatively large solid angles.

A structure is seen near the maximum p_{lab} for small angles in K^+p reactions. This is a consequence of Δ^{++} production. On the other hand there is no definite evidence for an enhancement corresponding to Δ^0 production in K^-p interactions, presumably because the corresponding small peak is masked by $N^{*0}_{\frac{1}{2}}$ production. The laboratory-momentum distributions of all the K^0 mesons shown in fig. 3 present the same feature.

2.3. *The p_L and $p_\perp$ distributions*

Recently Feynman [1] advocated the presentation of high-energy data in terms of the variables $x = p^*_L/p^*_{L\,max}$ and $p^2_\perp$. The distributions of x for the K^0 mesons in reactions (1) and (2) are shown in fig. 4. We see that K^+ and K^- data are similar in shape. The distributions are asymmetric around the axis $x = 0$; $d\sigma/dx$ decreases rapidly with increasing negative values of x and much more slowly for positive x values.

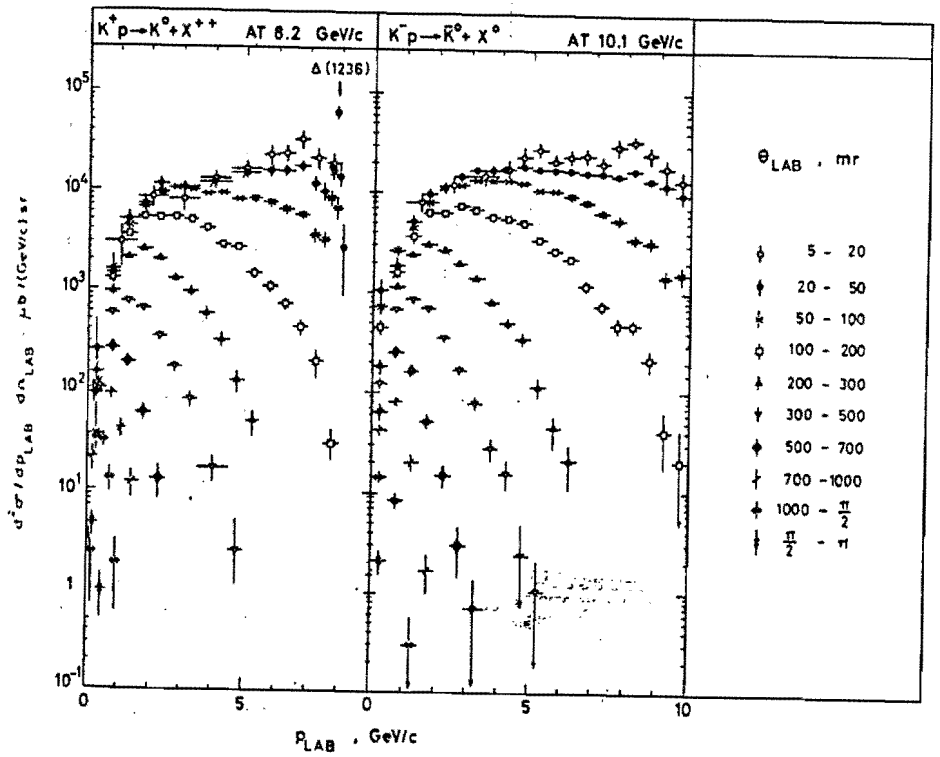

Fig. 2. Double-differential cross-section distribution $d^2\sigma/dp_{lab}\,d\Omega_{lab}$ for K^0 mesons produced in reactions (1) and (2).

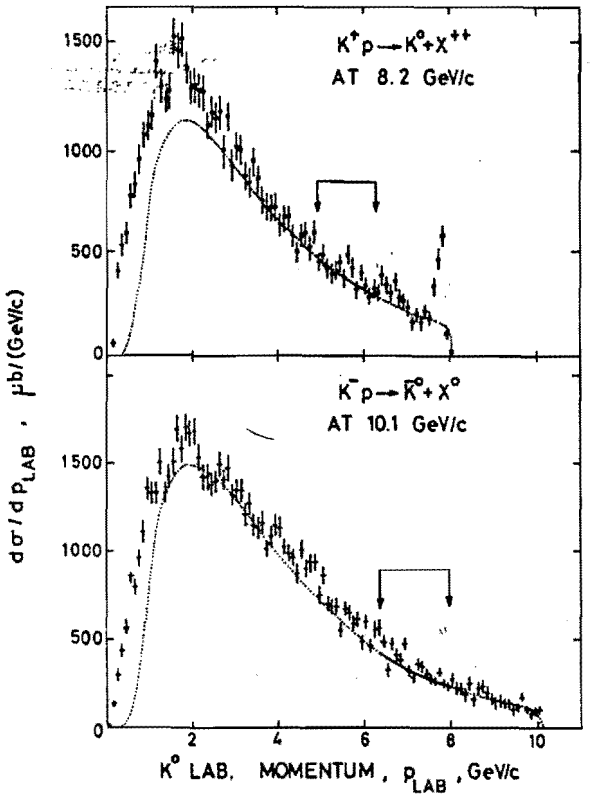

Fig. 3. K^0 lab momentum distributions for K^+ and K^- interactions. The lines represent the predictions of the parametrisation described in sect. 3. The solid lines are for the fitted region, the dotted lines for the extrapolation.

These $d\sigma/dx$ distributions for K^0 may be compared with those obtained for protons [3] and pions [4] produced in pp interactions. For protons, $d\sigma/dx$ is essentially flat, while for pions it decreases rapidly with increasing $|x|$. Thus, K^0 mesons present a behaviour intermediate between that of protons and pions, i.e., they tend to keep the momentum of the incident particle, but to a smaller extent than the protons.

It is interesting to note in fig. 4b that the $d\sigma/dx$ distributions for reaction (1) at 5 and 8.2 GeV/c are not only similar, but practically identical also in absolute value (no normalisation was made), at least for $-0.5 < x < +0.7$. This may be taken as evidence for the scaling behaviour predicted by Feynman [1], i.e. $d\sigma/dx$ distributions are energy independent, at least between 5 and 8.2 GeV/c for K^+p interactions.

In fig. 5 we present the distribution of $d\sigma/dp_\perp^2$ for K^0 mesons. The experimental results can be described satisfactorily both by an exponential function of p^2 and by the Cocconi-Koester-Perkins formula [5] in the region of $p_\perp^2 \leq 0.5$ (GeV/c)^2, which contains the great majority of the events.

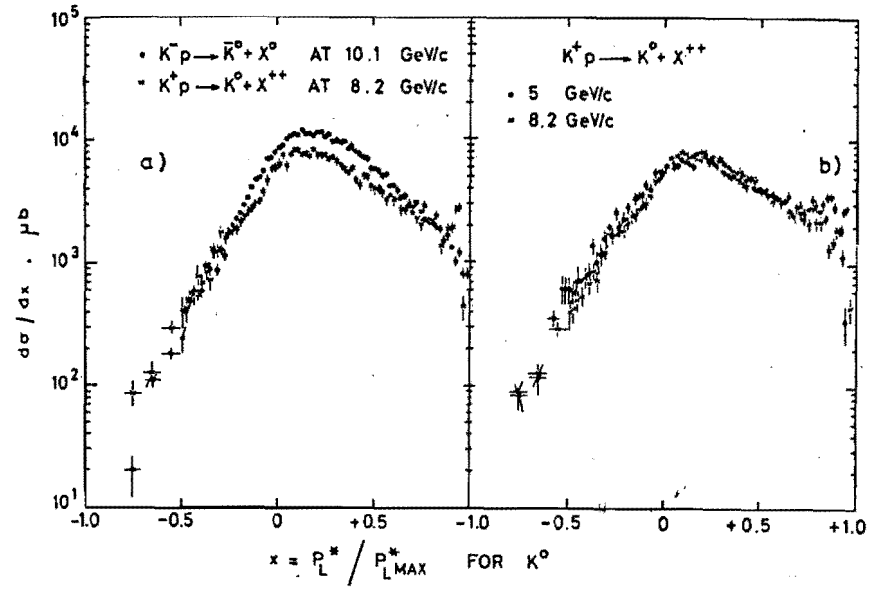

Fig. 4. Distribution of $d\sigma/dx$, where x is the c.m. longitudinal momentum of the K^0 meson divided by the maximum available momentum.

4. Missing mass spectra

Fig. 6 shows in a semi-logarithmic plot the mass spectrum of the system X in reactions (1) and (2). For low masses of X, enhancements are observed which are due to production of baryonic resonances. At higher masses, above about 2.0 GeV, however, it can be seen that the distributions are essentially smooth and consistent with an exponential shape. This higher mass region can be fitted with the formula

$$\frac{d\sigma}{dM} = \sigma_0 \, e^{kM} . \tag{3}$$

The values of the fitted slope k and of the normalisation constant σ_0, as well as the M-region over which formula (3) was fitted, are given in table 2. The same procedure was repeated for events with $t' \leq 1.0$ GeV^2 and the results are also given in the table.

In all the three cases investigated the slope k for the total sample of events has a value between 1.6 and 2.1 GeV^{-1}; for events with $t' \leq 1.0$ GeV^2 the value of k is somewhat lower and varies between 1.3 and 1.8 GeV^{-1}. There is a tendency for the value of k to decrease when the incoming energy decreases.

The fact that the mass spectrum of the system X is exponential is surprising since this distribution is a superposition of all the spectra corresponding to the various multiplicities in the final state, which, as can be seen in fig. 7 for some examples of 4C and 1C fitted channels, individually are by no means exponential and differ very much among themselves.

In order to study in more detail the mass distribution of the system X

Table 2
Fitted coefficients in formula (3), $d\sigma/dM = \sigma_0 e^{kM}$.

Reaction	Mass range (GeV)	t' range (GeV^2)	σ_0 ($\mu b/GeV$)	k (GeV^{-1})	χ^2/degrees of freedom
$K^+p \to K^0X^{++}$ at 5 GeV/c	2.0 - 2.5	All	40.6 ± 2.0	2.10 ± 0.05	21/8
		0 - 1.0	49.6 ± 2.4	1.81 ± 0.05	32/8
$K^+p \to K^0X^{++}$ at 8.2 GeV/c	2.0 - 3.45	All	17.1 ± 0.8	1.70 ± 0.05	47/27
		0 - 1.0	44.3 ± 2.1	1.33 ± 0.05	36/27
$K^-p \to \bar{K}^0X^0$ at 10.1 GeV/c	2.0 - 3.8	All	19.1 ± 0.9	1.65 ± 0.05	42/34
		0 - 1.0	34.1 ± 1.7	1.31 ± 0.05	42/34

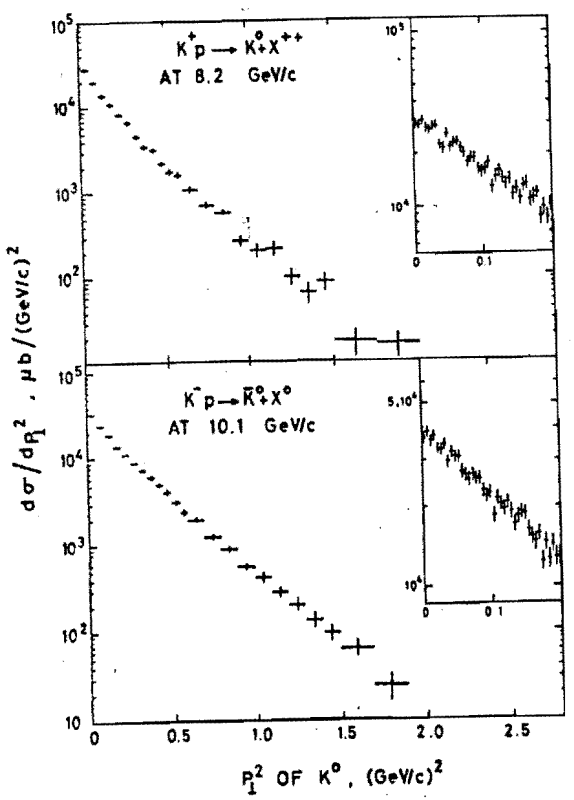

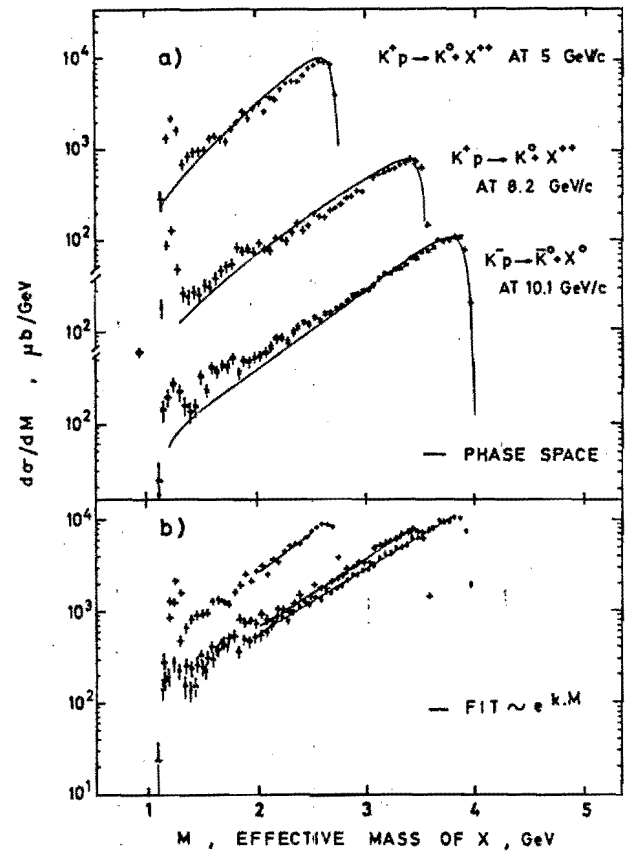

Fig. 6. Effective mass spectrum $d\sigma/dM$ of the system X in the reactions (1) and (2). The lines in fig. 6a represent the phase-space predictions. Those in fig. 6b are fits to the data with eq. (3).

We have calculated the phase-space mass distributions for systems consisting of a nucleon plus n pions (n ranging from 1 to 7) and then we have added them together under the assumption that for multi-neutral channels the relative probabilities of observing a given number of neutral particles are given by statistical isospin weights [6] applied to the cross sections of the 4C and 5C channels. It is interesting to see that the resulting curves shown in fig. 6, are roughly exponential in the M-regions specified in table 2. Thus the qualitative behaviour of the mass spectra in the region under discussion may appear as a first approximation a phase-space effect. One does not expect, however, phase space to provide by itself a satisfactory description of the data. Indeed it is well known that phase space grossly fails to describe the distributions that reflect the peripheral character of high-energy interactions, like $d\sigma/dt'$ (see next section) or p_L^* distributions.

As can be seen in fig. 6, for a fixed band of M-values we observe a strong energy dependence of the cross section: in the range from 5 to 10 GeV/c it

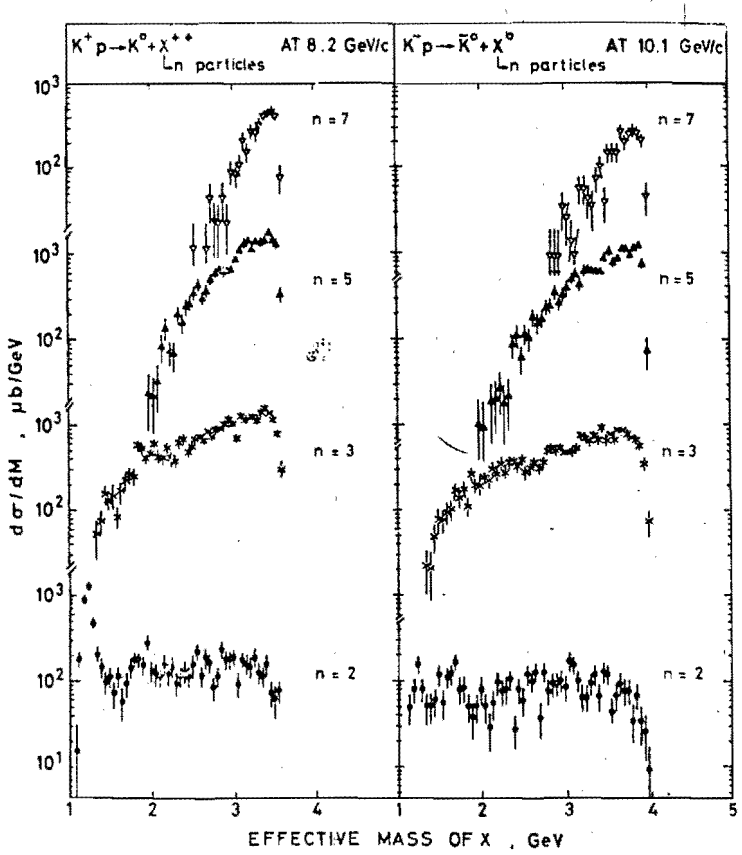

Fig. 7. Missing mass distributions $d\sigma/dM$ for different multiplicities in the final state.

decreases with increasing primary momentum ‡ approximately as $p_{lab}^{-2.5}$, similarly to what is observed for two-body charge-exchange reactions [7].

2.5. *Four-momentum-transfer distributions*

In fig. 8 are shown the $d\sigma/dt$ distributions of K^0 for both K^- and K^+ incident particles, and in fig. 9 the $d\sigma/dt'$ distributions. It may be seen that the general shape of the t and t' distributions of the K^0 mesons produced in K^- and K^+ interactions are similar and greatly at variance with phase space predictions (dashed lines in fig. 9) in the region $0 < t' < 2.0$ GeV^2 which contains 80% of the events.

The t' distributions for different mass bands of X are presented in fig. In the small t' ($t' \leq 1.0$ GeV^2) region they are consistent with the exponential

$$\left(\frac{d\sigma}{dt'}\right)_{M=\text{const}} = (\text{const})\, e^{-At'} .$$

‡ Preliminary results for 16 GeV/c K^+p interactions confirm this $p_{lab}^{-2.5}$ dependence.

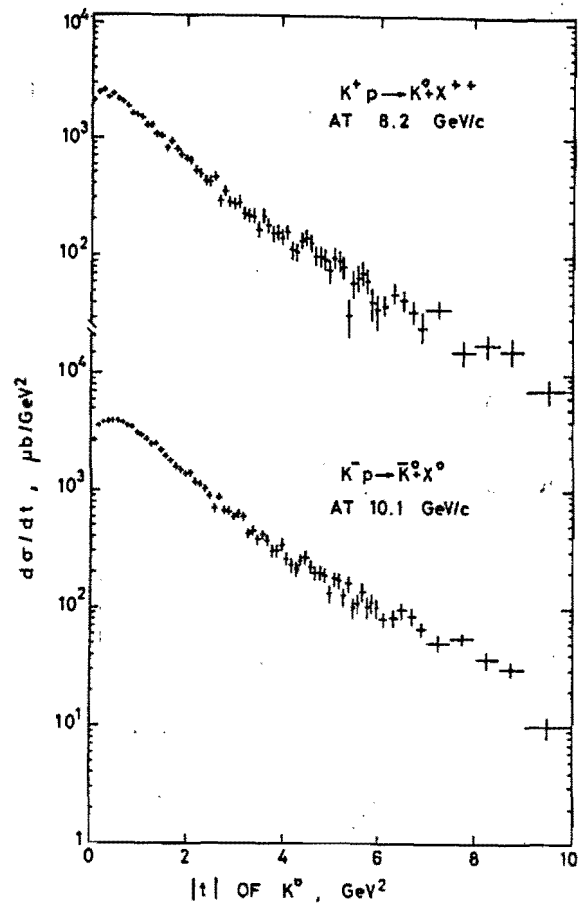

Fig. 8. Distribution of the squared four-momentum transfer from incident kaon to produced K^0.

The fitted values of the parameter A for each mass interval of 100 MeV in the region $0 \leq t' \leq 1.0$ GeV^2, are presented in figs. 11a and 11b. Again there is no significant difference between K^- and K^+-induced reactions. The combined K^+ and K^- data are presented in fig. 11c. The decrease of the exponential slope with increasing mass of the system produced, reported in several experiments of hadron collisions and photoproduction, is clearly confirmed here. The combined data for the variation of A with mass have been fitted with the relation

$$A = c\left(\frac{M}{M_0}\right)^{-\alpha}, \qquad M_0 = 1 \text{ GeV} \tag{5}$$

and values of $c = 26.4 \pm 2.5$ GeV^{-2} and of $\alpha = 2.34 \pm 0.12$ were obtained.

It is known that π^+p interactions at 8 GeV/c can be well described by a simple model where the transition matrix element depends only on the four-

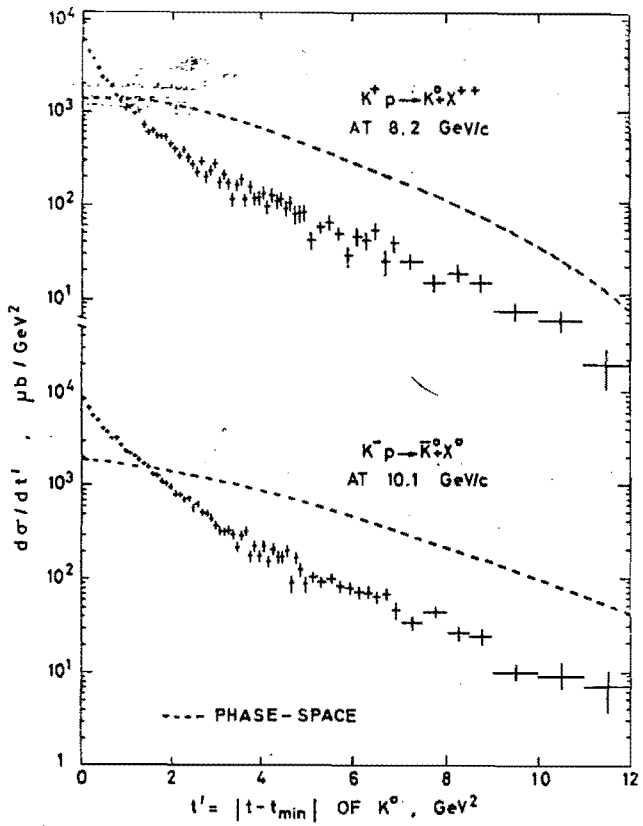

Fig. 9. The $t' = |t - t_{min}|$ distributions of K^0. The dashed lines are the predictions of phase space normalised to the total number of events.

momentum transfer to the nucleon [8]. In that case of πp interactions at the relatively low momentum of 8 GeV/c, the leading π-meson is lost among the various pions produced. The situation we are considering here is different. In reactions (1) and (2) the outgoing K^0 has strangeness and mass different from those of the produced pions and therefore tends to conserve its identity of primary particle. We can expect therefore that the production characteristics of the K^0 mesons will be more similar to those of protons than to those of pions, and thus that the matrix element will not depend only on the momentum transfer to the proton. We have nevertheless checked whether is possible to describe reactions (1) and (2) assuming that the matrix element squared of these processes depends only on the four-momentum transfer from the incoming to the outgoing nucleon. The dashed line in fig. 11c gives the result of the calculation of the exponential slope of the t' distributions. As it can be seen, the values predicted for the parameter A are in drastic disagreement with experiment.

2.6. K^* *production in reactions* (1) *and* (2)

In a missing mass experiment of this kind, one is led to visualise the K^0

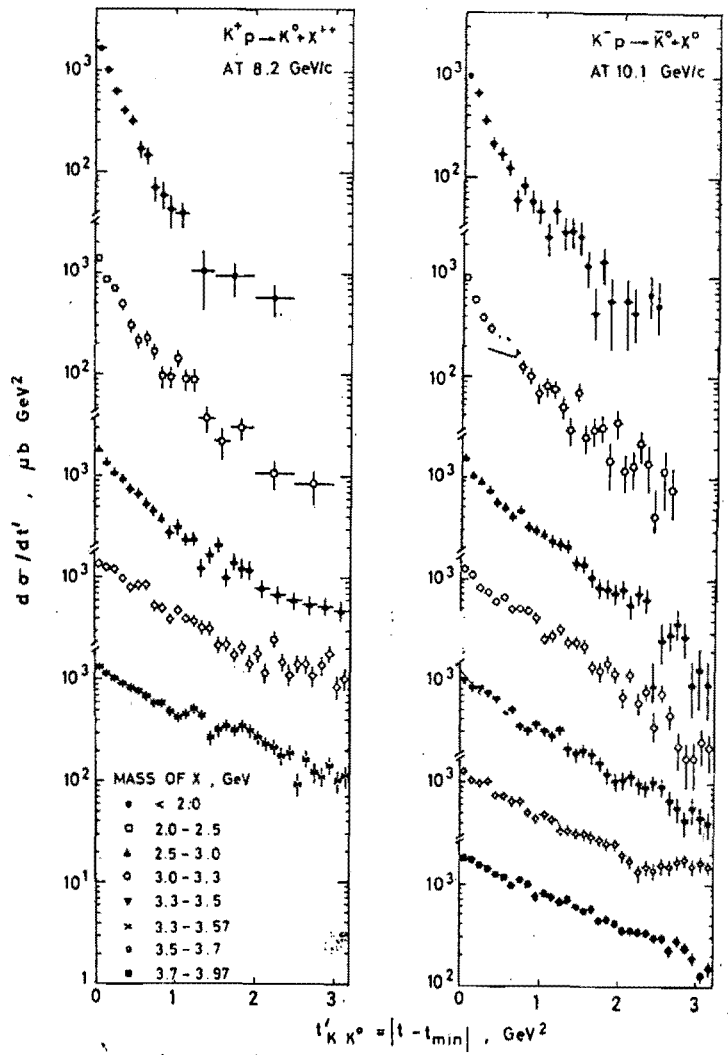

Fig. 10. The $t' = |t - t_{min}|$ distributions of K^0 for different mass bands of the system X.

is produced alone at one interaction vertex not correlated with the particles contained in the X-system. This does not, obviously, correspond to reality. In particular, an important fraction of the K^0 mesons must derive from the decay of K^* resonances. In fig. 12 are presented the $(K^0\pi^+)$ effective-mass spectrum for reaction (1) and the $(\bar{K}^0\pi^-)$ effective mass spectrum for reaction (2). In both distributions one can see a strong $K^*(890)$ peak, that includes about 25% of the K^0 mesons. We estimated that, in total about 40% of the K^0 mesons produced at 8 to 10 GeV/c derive from the known K^* resonances, both in charged and neutral states. Since $K^*(890)$ gives the largest contribution, we have verified that the general behaviour of the K^0 deriving from the $K^*(890)$ mass band is similar to the behaviour of the K^0 from mass

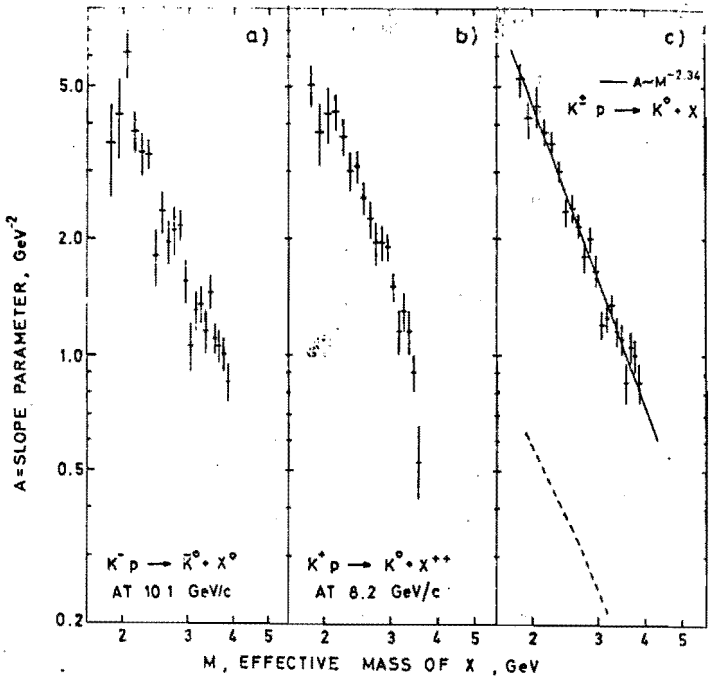

Fig. 11. Values of A when $e^{-At'}$ is fitted to the $d\sigma/dt'$ distributions, (a) for the reaction $K^-p \to \bar{K}^0X^0$ at 10.1 GeV/c, (b) for the reaction $K^+p \to K^0X^{++}$ at 8.2 GeV/c, and (c) for the sum of both experiments. The solid line is the fit with $A = c(M/M_0)^{-\alpha}$. The dashed line represents the calculation described in subsect. 2.5.

bands adjacent to $K^*(890)$ in the $(K^0\pi)$ system. Therefore, we conclude that the general behaviour of the K^0 is not greatly affected by resonance production.

3. PARAMETRISATION OF THE DATA

We have shown that for small t' values ($t' \leq 1.0$ GeV^2), the t' dependence of the cross section for each narrow band of the mass M is described by the empirical formula (3), and the M-dependence of the exponential slope A is described by the function (5). As one can see in fig. 10, the t' distribution is well described by our exponential fits also for t' values somewhat larger than 1.0 GeV^2. Therefore we can try to extend our parametrisation over the whole kinematically allowed region. The double differential cross section may then be written in the form:

$$\frac{d^2\sigma}{dt'\,dM} = f(M)\exp\left[-c\left(\frac{M}{M_0}\right)^{-\alpha} t'\right]. \qquad (7)$$

Formula (3), which gives the $d\sigma/dM$ parametrisation, is the result of the integration of formula (7) over t' $t' \leq 1.0$ GeV^2. Combining formulae (3) and

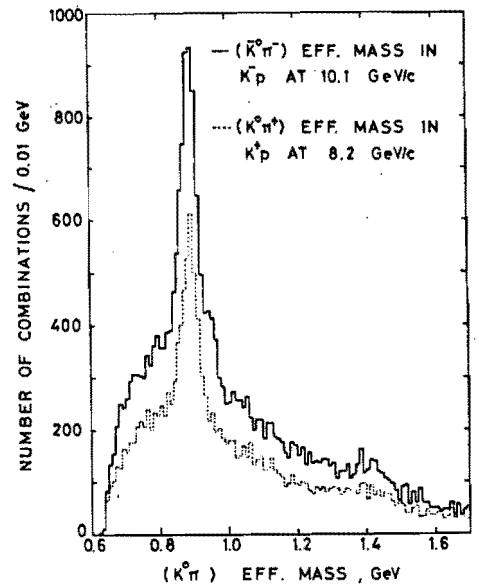

Fig. 12. Effective mass of the system $(K^0\pi)$ for K^+ and K^- interactions.

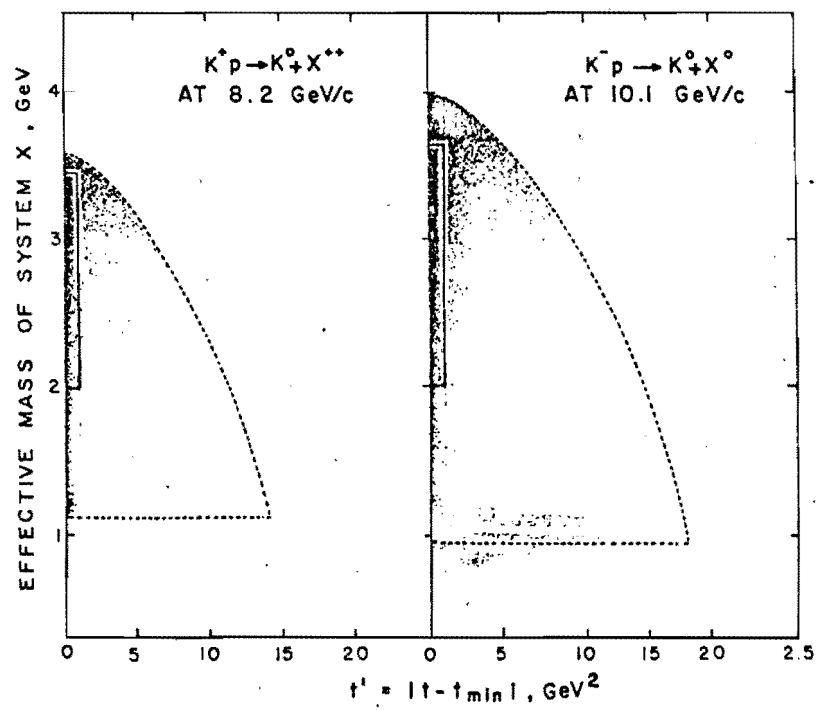

Fig. 13. Two-dimensional plot of t' versus M for all K^0 events in reactions (1) and (2). The solid lines delimit the region in which formulae (3) and (4) have been fitted

$$\frac{d^2\sigma}{dt'\,dM} = \sigma_0\, c \left(\frac{M}{M_0}\right)^{-\alpha} \frac{\exp[kM - c(M/M_0)^{-\alpha} t']}{1 - \exp[-c(M/M_0)^{-\alpha}]},$$

where the parameters σ_0 and k are the constants given in table 2. The region of strict validity of this formula is limited to the same range of M as for eq. (3), i.e. 2.0 - 2.5 GeV and 2.0 - 3.45 GeV for K^+p reactions at 5 and 8.2 GeV/c, respectively, and 2.0 - 3.8 GeV for 10.1 GeV/c K^-p reactions.

The limits of strict validity of the parametrisations are shown in fig. 2 by the solid lines delimiting rectangular regions in the plots of M versus t'. Though these rectangles cover a small fraction of the kinematically allowed areas, the events are strongly concentrated in the region of large M and small t', so that, for both K^+ and K^- reactions, the rectangles contain approximately 50% of the total events. As an example of the accuracy of the parametrisation of eq. (8) in describing the data, we show in fig. 3 the calculated distribution of $d\sigma/dp_{lab}$. The curve is drawn as a solid line for the p_{lab} region where eq. (8) is strictly valid and as a dotted line for the extrapolated regions. As can be seen in fig. 3, the solid line covers a very small range of p_{lab} and the extrapolations at high momenta and at low momenta down to about 2 GeV/c satisfactory describe about 80% of the events. Disagreement is noted, however, specially in fig. 3a, in the high momentum range, at the values of p_{lab} which correspond to baryonic resonances production (mostly $\Delta(1236)$). Besides, for momenta below $\approx$ 2 GeV/c, the parametrisation is definitely inadequate; this region corresponds to K^0 mesons produced backwards in the c.m. system.

All the other experimental distributions presented in this paper have been compared with the predictions of parametrisation (8). The results are not shown here, because the situation is always the same as described for fig. 3, namely that the description is adequate, except for baryonic resonance production and backward emitted K^0 mesons.

6. CONCLUSIONS

In the study of 5 and 8.2 GeV/c K^+p and 10.1 GeV/c K^-p interactions containing a K^0 in the final state plus the system X of any other particles, the following results were obtained:

(a) There is no qualitative difference, apart from absolute cross sections, in the production characteristic of K^0 by K^- and K^+ mesons.

(b) There is no strong energy dependence for the probability of the inelastic charge-exchange reactions, i.e., the fraction of the inelastic reactions giving K^0 mesons is approximately constant between 3 and 10 GeV/c and equal to about 40% of the total inelastic cross section.

(c) The distribution of the effective mass of the system X is exponential for $M \geq 2.0$ GeV, in all cases studied.

(d) The $d\sigma/dt'$ distributions for a given band of the mass of X can be fitted for small t' values, with an exponential $\exp(-At')$; the parameter A of the exponential decreases with increasing values of the mass as

$$\left(\frac{M}{M_0}\right)^{-\alpha}, \qquad \text{with } \alpha \approx 2.$$

(e) For a fixed band of M, we observe a strong energy dependence of the cross section, which in the range from 5 to 10 GeV/c decreases with the increasing primary momentum approximately as $p_{lab}^{-2.5}$, similarly to what is observed for two-body charge-exchange reactions.

(f) The values of the parameter A of the $d\sigma/dt'$ distributions are much larger than those expected from the peripheral production of nucleons.

(g) The production of K^* resonances does not affect significantly the general behaviour of the K^0 mesons.

(h) About 80% of the data are reasonably described by the two-dimensional parametrisation in t' and M given by eq. (8), deduced from fits describing about 50% of the events.

It would be of great interest to compare these results with the limiting fragmentation model [9], Feynman's ideas [1] or the thermodynamical model of Hagedorn [10]. Unfortunately, at present, these predictions are not available in a form which may be directly compared with our experimental data.

We are indebted to the operating crews of the CERN proton-synchrotron, 150 cm British, 80 cm and 200 cm CERN hydrogen bubble chambers and to the constructors of the beams. We would like to thank the scanning, measuring and computing staff of each of our laboratories. We are pleased to acknowledge helpful discussions with Dr. R. Armenteros and Professor M. Peyrou.

REFERENCES

[1] R.P. Feynman, Phys. Rev. Letters 23 (1969) 1415.
[2] R.L. Cool et al., Phys. Rev. Letters 17 (1966) 102;
W. Galbraith et al., Phys. Rev. 138 (1965) 913;
E. Flaminio, J.D. Hansen, D.R.O. Morrison and N. Tovey, Compilation of cross sections, CERN/HERA reports 70-6, 70-7.
[3] E.W. Anderson et al., Phys. Rev. Letters 19 (1967) 198.
[4] H. Bøggild et al., Scandinavian Bubble Chamber Collaboration, Nucl. Phys. B27 (1971) 285.
[5] G. Cocconi, L.J. Koester and D.H. Perkins, UCRL 10022 (1961) p. 167.
[6] J. Bartke, Statistical model and cross sections for high-energy reactions, Herceg-Novi report (1970).
[7] D.R.O. Morrison, Phys. Letters 22 (1966) 528.
[8] T. Hofmokl et al., Nucl. Phys. B4 (1968) 573.
[9] J. Benecke, T.T. Chou, C.N. Yang and E. Yen, Phys. Rev. 188 (1969) 2153;
H. Cheng and T.T. Wu, Phys. Rev. Letters 23 (1969) 1311.
[10] R. Hagedorn, Nuovo Cimento 56A (1968) 1027.

Proposal No. 383

Scientific Spokesman:

H. G. E. Kobrak
University of California, San Diego
(714) 452-3268
FTS Operator (714) 293-5000
At Fermilab ext. 3056/4198

Addendum to

A PROPOSAL TO STUDY THE INCLUSIVE PRODUCTION OF K_S^0 BY K^- ON HYDROGEN

H.G.E. Kobrak, R.E. Pitt, R.A. Swanson

University of California, San Diego

La Jolla, CA. 92037

August 1975

ABSTRACT.

This addendum represents a detailed look at the physics and analysis which is presented more concisely in the main body of proposal P-383.

We argue here that Mueller analysis and Regge theory have made inclusive reactions an important tool in the study of stron interactions.There have been many inclusive experiments done at Fermilab and elsewhere,but their usefulness has been limited by one or more of the following:

1.)The kinematic region (x,s,t) is not appropriate to the Mueller-Regge analysis.
2.)The experiment lacks the statistical power to make definite tests.
3.)The experiment uses a reaction whose complexity in terms of Regge exchanges excludes any meaningful test or application of the theory.

The experiment we propose here is in the right kinematic region,has high statistical power and can be analyzed in terms of the ρ-trajectory and its exchange degenerate partner the A_2.In addition to making definite studies of the Mueller-Regge type,the joint analysis of this experiment with the inclusive pion charge exchange (E-350) and inclusive kaon scattering (e-118A) experiments permits additional conclusions unavailable from any single experiment.

As part of this addendum we present a proposal for a high intensity high momentum charged tagged beam for the M4 line.It is economical to install and very easy to convert back to a neutral beam and should have a $\pi^-:K^-:\bar{P}$ ratio of 20:5:1 at 100 Gev/c.

I. INTRODUCTION

One approach in the phenomenology of particle interactions at high energies is the description of scattering amplitudes in terms of their singularities and residues in the complex angular momentum plane. This approach, called Regge theory, is attractive to the extent that singularities are dominated by simple poles.

The best way to obtain specific information about the structure of scattering amplitudes is to carry out those experiments which isolate single Regge exchanges. One can study trajectories and test for cut contributions, violation of exchange degeneracy, factorization, etc. in a relatively simple situation. The physical interpretation is then highly constrained, and deviations from the predictions are not masked by the degrees of freedom inherent in a multiparameter fit. The problems of multiparameter fits are discussed in the analysis of $P + P \rightarrow P + X$ by Field and Fox[1], where several choices of the possible exchanged trajectories are shown to fit the data reasonably well.

In Table I we show the completed Fermilab experiments which meet our criterion of simple exchange structure

Experiment	Description	Exchange
82	$K_L + C \rightarrow K_S + C$	ω
104	Particle/Antiparticle differences of (π,p), (K,p) and (p,p) total cross sections	ω, ρ
111	$\pi^- + p \rightarrow \pi^0 + n$	ρ
	$\pi^- + p \rightarrow \eta^0 + n$	A_2

In each case the experiment involves the exchange of a single trajectory, or there is a linear combination of measured cross sections which can be described by a single exchange.

The experiment we propose here,

$$K^- + p \rightarrow \overline{K^0} + X$$
$$\hookrightarrow K_s$$

studies a process involving only the exchanges of ρ and A_2, which appear to be an exchange degenerate pair of trajectories. By itself, and in conjunction with other Fermilab experiments, it opens the door to a number of tests of ordinary and triple Regge theory, factorization and SU_3, exchange degeneracy and the measurement of Reggeon-proton cross sections. The high cross section for the inclusive process yields a statistical accuracy unobtainable in exclusive reactions. We cover a region in S, x and t inaccessible to previous kaon charge exchange experiments.

The exchange of K* or baryon trajectories occurs in processes where a K^0 or Λ final state is produced by an incident pion or antiproton. While such processes are not the subject of this proposal, we are able to tag pions and antiprotons in the incident beam, and it is likely that the data system has enough capacity to allow taking pion and antiproton interactions concurrently with the kaon interactions. In this way, we expect to gather preliminary data on a number of additional processes which may be the subject of future proposals.

II. INCLUSIVE REACTION PHYSICS

In this section we discuss some of the physics which can be extracted from some of the kaon charge exchange data. We estimate cross sections, data collection rates and measurement errors on some quantities of interest.

To study the process

$$K^- + P \rightarrow \overline{K^0} + X$$

with 4-momenta

$$p_1 + p_2 \rightarrow p_3 + p_4$$

we use the customary variables

$$s = (p_1 + p_2)^2$$

$$t = (p_1 - p_3)^2$$

$$M^2 = p_4^2 = (p_1 + p_2 - p_3)^3 = t + m_2^2 + 2m_2(E_1 - E_3)$$

For large s and small t, useful relations are

$$s = 2m_2E_1$$

$$x = E_3/E_1$$

$$M^2 + t + m_2^2 + s(1 - x)$$

where E_1 and E_3 are the laboratory energies of charged and neutral kaon respectively.

We will collect data in the region

$$40 < s < 300 \text{ GeV}^2$$
$$-3 < t < 0 \quad (\text{GeV}/c)^2$$
$$0.8 < x < 1.0$$

These limits are determined by the range of applicability of Regge theory, available flux in the M4 beam line and good detection efficiency of our equipment. While the range in s is determined by the range of beam momentum and the range in t by the cross section, the range in x depends mostly on the detector arrangement. When the detector is optimized for the range $0.8 < x < 1.0$, enough data will be collected for $x < 0.8$ to study the scattering amplitude as one leaves the "triple Regge region."

As discussed in our proposal P-383, one can use the Mueller generalized optical theorem and Regge theory to show that in the above region the inclusive cross section can be written

$$\frac{d^2\sigma}{dtdx} = \sum_{ijk} F_{ijk}(t) \left(\frac{s}{M^2}\right)^{\alpha_i(t) + \alpha_j(t) - 1} (M^2)^{\alpha_k(0) - 1}$$

where $F_{ijk}(t)$ is a collection of Regge residues and signature factors, i and j refer to all allowed exchanged trajectories and k enters from the Regge description of the Reggeon-proton total cross section.

This remarkable result has been known for about four years, but has been subjected to only the most rudimentary experimental tests. Data on

inclusive kaon charge exchange amount to a few thousand events at 8 GeV and 14.3 GeV. Most of them are outside the triple Regge region. There is a large amount of data for $P + P \to P + X$, but as mentioned before, the multiplicity of allowed exchanges permits only very general conclusions to be drawn. All of these data are in general agreement with the predictions of triple Regge theory and have been used to estimate our data rates.

Our numerical estimates are made for a single exchange degenerate Regge trajectory

$$\alpha_R(t) = \alpha_o + \beta t = 0.55 + 0.925\ t$$

and for the Pomeron trajectory

$$\alpha_p(t) = 1$$

In that case, the expression for the inclusive cross section becomes

$$\frac{d^2\sigma}{dtdx} = F_{RRP}(t)\left(\frac{s}{M^2}\right)^{2\alpha_R(t) - 1} (M^2)^{\alpha_p(0) - 1}$$
$$+ F_{RRR}(t)\left(\frac{s}{M^2}\right)^{2\alpha_R(t) - 1} (M^2)^{\alpha_R(0) - 1}$$

With the abovementioned numerical values we get

$$\frac{d^2\sigma}{dtdx} = F_{RRP}(t)\ (1 - x)^{-0.1 - 1.85t}$$

$$+\ F_{RRR}(t)\ \frac{1}{\sqrt{s}}\ (1 - x)^{-0.55 - 1.85t}$$

From inclusive kaon charge exchange data at 14.3 GeV/c we estimate

$$F_{RRP}(t) = 4.4 \text{ mb/(GeV/c)}^2$$

$$\frac{1}{\sqrt{s}} F_{RRR}(t) < 0.8 \text{ mb/(GeV/c)}^2$$

Because of the $1/\sqrt{s}$ dependence of the RRR term, we ignore its contribution to the rate estimates at the higher Fermilab values of s. See Appendix I for typical rate estimates from the RRP term alone.

The proposed experiment will generate a data sample of several million events in the (x,t) region appropriate for the triple Regge analysis. The following are possible approaches to such an analysis.

1) Measurement of ρ and A_2 Regge trajectories.

For $M^2 \ll s$, ordinary Regge theory gives as an expression for the cross section

$$\frac{d^2\sigma}{dtdx} = F(t,M^2)\, s^{2\alpha(t) - 1}$$

corresponding to the diagram

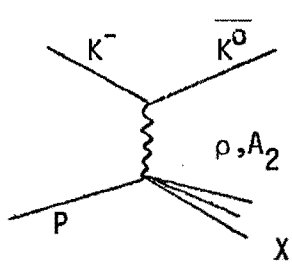

the s-dependence of the cross section at fixed t and M^2 will yield $\alpha(t)$ for $-3 < t < 0$ $(GeV/c)^2$. The errors on $\alpha(t)$ also depend on t; a 100 hour run with 50 and 100 GeV/c K^- will yield an error in $\alpha(t)$ of about 0.01 at $t = -1$ $(GeV/c)^2$, where $\alpha(t)$ is expected to be about -0.4. There are of course other ways of extracting $\alpha(t)$ from the data, but this is probably the most direct one.

2) Combined analysis of inclusive kaon charge exchange (P383) and inclusive pion charge exchange (E350)

Exchange degeneracy, SU_3 and factorization predict that

$$\left.\frac{d^2\sigma}{dtdx}\right)_{\pi^- p\to\pi^0 X} = 2\sin^2\left(\frac{\pi\alpha(t)}{2}\right)\left.\frac{d^2\sigma}{dtdx}\right)_{K^- p\to\bar{K}^0 X}$$

$$\left.\frac{d^2\sigma}{dtdx}\right)_{\pi^- p\to\eta X} = \frac{2}{3}\cos^2\left(\frac{\pi\alpha(t)}{2}\right)\left.\frac{d^2\sigma}{dtdx}\right)_{K^- p\to\bar{K}^0 X}$$

where $\alpha(t)$ can be determined either from kaon or pion charge exchange data. Because of the existence of zeroes of the Regge signature factor, the t-dependence of deviation from the above relations can be used to diagnose their origin. If only ρ and A_2 trajectories are degenerate, one has the weaker condition

$$\left.\frac{d^2\sigma}{dtdx}\right)_{\pi^- p\to\pi^0 X} + 3\left.\frac{d^2\sigma}{dtdx}\right)_{\pi^- p\to\eta X} = 2\left.\frac{d^2\sigma}{dtdx}\right)_{K^- p\to\bar{K}^0 X}$$

3) Combined analysis of inclusive kaon charge exchange (P383) and inclusive charged kaon scattering (E118A)

The analysis of the process

$$K^{\pm} + p \rightarrow K^{\pm} + X$$

in progress at the single arm spectrometer facility, will involve the Pomeron, ω, f, ρ and A_2. According to Finkelstein and Rajaraman[2] isospin symmetry allows one to subtract the ρ, A_2 terms of

$$\left.\frac{d^2\sigma}{dtdx}\right)_{K^-p\rightarrow K^0X} \quad \text{from} \quad \left.\frac{d^2\sigma}{dtdx}\right)_{K^{\pm}p\rightarrow K^{\pm}X}$$

By assuming complete exchange degeneracy of ρ, A_2, ω and f, one can subtract all by the PPP, PRP, PPR AND PRR vertices. The latter two go as $S^{-\frac{1}{2}}$, so we will get a relatively unobstructed view of the triple Pomeron vertex from the remaining PPP and PRP terms.

4) Relative amounts of RRP and RRR couplings.

As noted in paragraph 1), at fixed t and M^2 $\frac{d^2\sigma}{dtdx}$ varies as $S^{2\alpha(t)-1}$. If we fix t and x, we have

$$\frac{d^2\sigma}{dtdx} = f_{RRP}(t,x)S^{\alpha_p(0)-1} + f_{RRR}(t,x)\, S^{\alpha_R(0)-1}$$

$$\cong f_{RRP}(t,x) + \frac{1}{\sqrt{s}} f_{RRR}(t,x)$$

To the extent that $\alpha_p(t)$ behaves like a simple pole with $\alpha_p(0) = 1$, we should be able to identify RRR terms down to about 1% of the dominant RRP term.

5) Test for exchange degeneracy and interference terms.

If $\alpha_\rho(t) = \alpha_{A_2}(t)$ (weak exchange degeneracy), the Regge signature factors make all $\rho - A_2$ interference terms identically zero. Such terms are also distinguished by being odd under charge conjugation, and hence are the only terms to change sign when comparing $K^{\pm}+p \to K^0+X^{++}$ with $K^-+p \to \overline{K^0}+X^0$ in the triple Regge region. Such terms are RRR, whose contribution is largest at small values of s. We therefore propose to take some data on $K^+ + p \to K^0 + X^{++}$ at $S = 100\ (\mathrm{GeV/c})^2$ ($p_K = 50$ GeV/c) in order to compare with data on $K^- + p \to \overline{K^0} + X^0$ for the same beam energy. Any difference would be evidence of $\rho - A_2$ interference.

6) The preceding analyses have all assumed the validity of Triple Regge Theory. Since the ρ-trajectory has been measured for $-1 < t < 0\ (\mathrm{GeV/c})^2$ by pion charge exchange (E-111), we are able to predict the dependence of $d^2\sigma/dtdx$ on s,t and M^2. All of these predictions involve the same $\alpha(t)$, so we can test the validity of Triple Regge Theory internally by determining $\alpha(t)$ by several different types of analysis (see paragraph 1, and Appendix I, for example).

7) As shown by Finkelstein and Rajaraman[2], $d^2\sigma/dtdx$ can be written in terms of a $KK\rho$ residue function (determined from exclusive scattering or from the Veneziano Model) and the Reggeon-proton total cross section. We are therefore able to measure the Reggeon-proton total cross section as a function of Reggeon mass $\sqrt{t}$ and M.

APPENDIX I

We estimate data rates and cross sections as follows:

1) The t-dependence of either RRP or RRR is of the form

$$\frac{d^2\sigma}{dtdx} \sim F(t)\ (1 - x)^{-2\beta t} \quad ; \quad \beta = 0.925$$

From $K^+ + p \rightarrow K^0 + X^{++}$ data at 8 GeV/c, we find $F(t)$ = const for $-1.0 < t < 0\ (\mathrm{GeV/c})^2$ to about 10% (see Figure I).

2) With the above approximation for $F(t)$, we can integrate $\frac{d^2\sigma}{dtdx}$ over t

$$\int_{-00}^{0} \frac{d^2\sigma}{dtdx}\, dt = \left[F_{RRP}\ (1 - x)^{1-2\alpha_o} + \frac{F_{RRR}}{S^{1-\ o}}\ (1 - x)^{-\alpha_o} \right] \int_{-\infty}^{0} dt\ (1 - x)^{-2\beta t}$$

$$= \left[F_{RRP}\ (1 - x)^{1-2\alpha_o} + \frac{F_{RRR}}{S^{1-\ o}}\ (1 - x)^{-\alpha_o} \right] \left[\frac{-1}{2\beta\ \ln(1-x)} \right]$$

on comparing the above distribution with data for $K^- + p \rightarrow \overline{K^0} + X$ at 14.3 GeV/c, we find the data consistent with

$$F_{RRP} = 4.4\ \frac{\mathrm{mb}}{(\mathrm{GeV/c})^2} \quad ; \quad \frac{F_{RRR}}{\sqrt{s}} \cong 0\ \frac{\mathrm{mb}}{(\mathrm{GeV/c})^2}$$

(see Figure II)

Since the RRP term is independent of S and the RRR term goes as $S^{-\frac{1}{2}}$, we estimate cross sections at higher energies using the above values.

Table II gives the cross sections and rates for bins of

$$\Delta t = 0.2\ (\mathrm{GeV}/c)^2$$

and $\Delta x = 0.1$

at

$$p_K = 100\ \mathrm{GeV}/c\ (S = 200\ \mathrm{GeV}^2)$$

For each bin, the first entry is $\Delta\sigma = \int_{\Delta t} dt \int_{\Delta x} dx \frac{d^2\sigma}{dtdx}$ in μb, and the second entry is the number of events expected in the bin for a 100 hour run with $4 \times 10^5 K^-$ per pulse on a 0.3 m hydrogen target (43 events/μb/hour). We estimate an average 50% detection efficiency; one third of the neutral kaons decay to two charged pions.

The last two rows have the value of $\alpha(t)$ and its error, for the conditions specified, when $\alpha(t)$ is determined by fitting the x-dependence of $\frac{d^2\sigma}{dtdx}$

x \ -t	.1	.5	.9	1.3	1.7	2.1
.95	68 295 K	7.4 32 K	.81 3.5 K	.090 390	.0096 40	.0010 4
.85	75 324 K	18.4 80 K	4.5 19 K	1.11 4.8 K	.27 1.2 K	.066 285
.75	78 337 K	28.0 121 K	10.1 43.5 K	3.6 15.5 K	1.29 5.6 K	.46 2.0 K
$\alpha(t)$	.46	.09	-.28	-.65	-1.02	-1.39
Estimated error in $\alpha(t)$	.001	.003	.008	.024	.073	.23

REFERENCES

1. R. D. Field and G. C. Fox, Nuclear Physics, B80, 367 (1974).

2. J. Finkelstein and R. Rajaraman, Physical Review, D5, 672 (1972).

Figure I.

Estimate of F(t) from data on $K^+P \rightarrow K^oX^{++}$ at 8 GeV/c

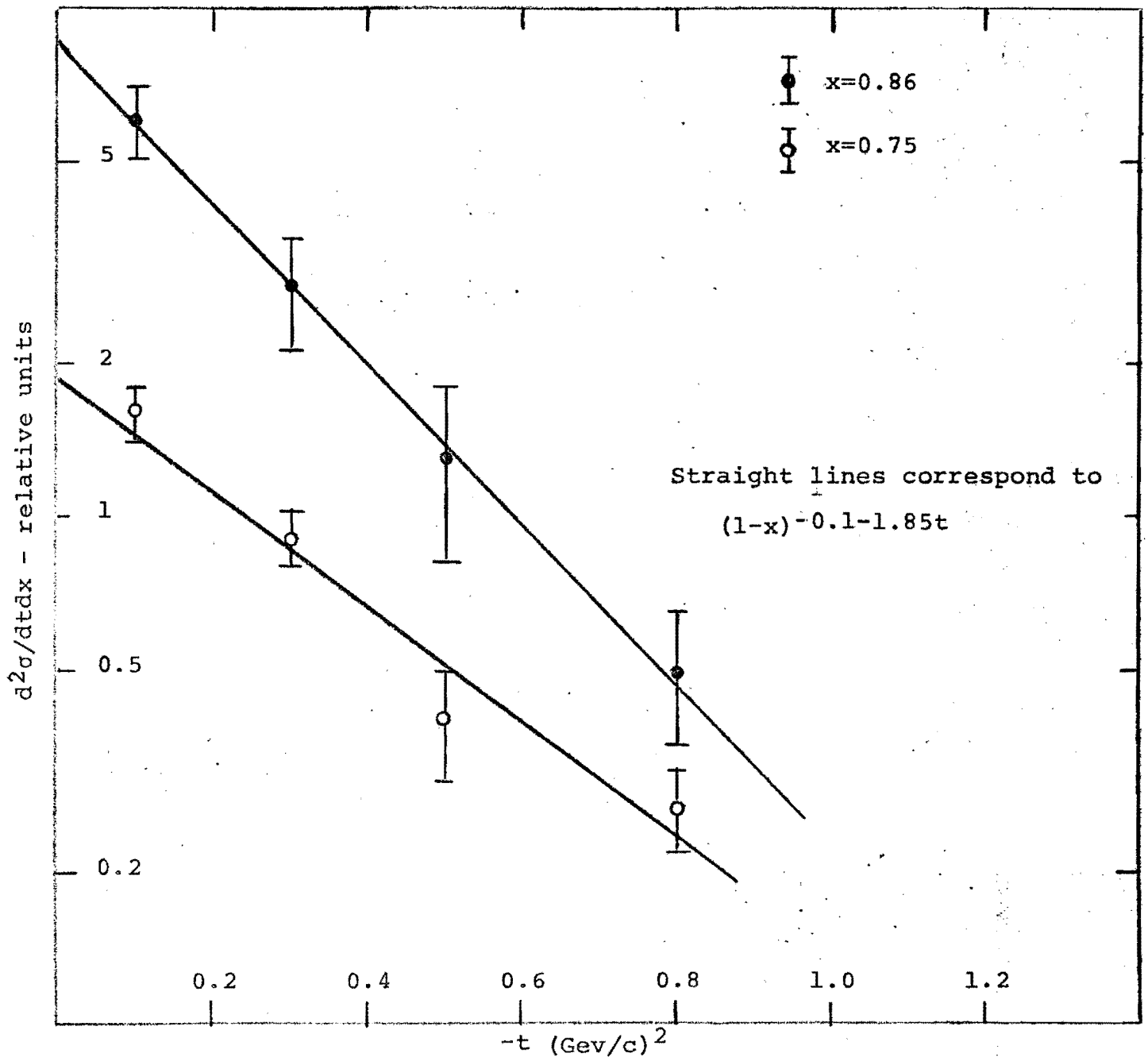

Conclusion: F(t)=constant, since no additional t-dependence is needed to fit the data.

Figure II.

Estimate of F_{RRR} from data on $K^-P \to K^oX^o$ at 14.3 GeV/c

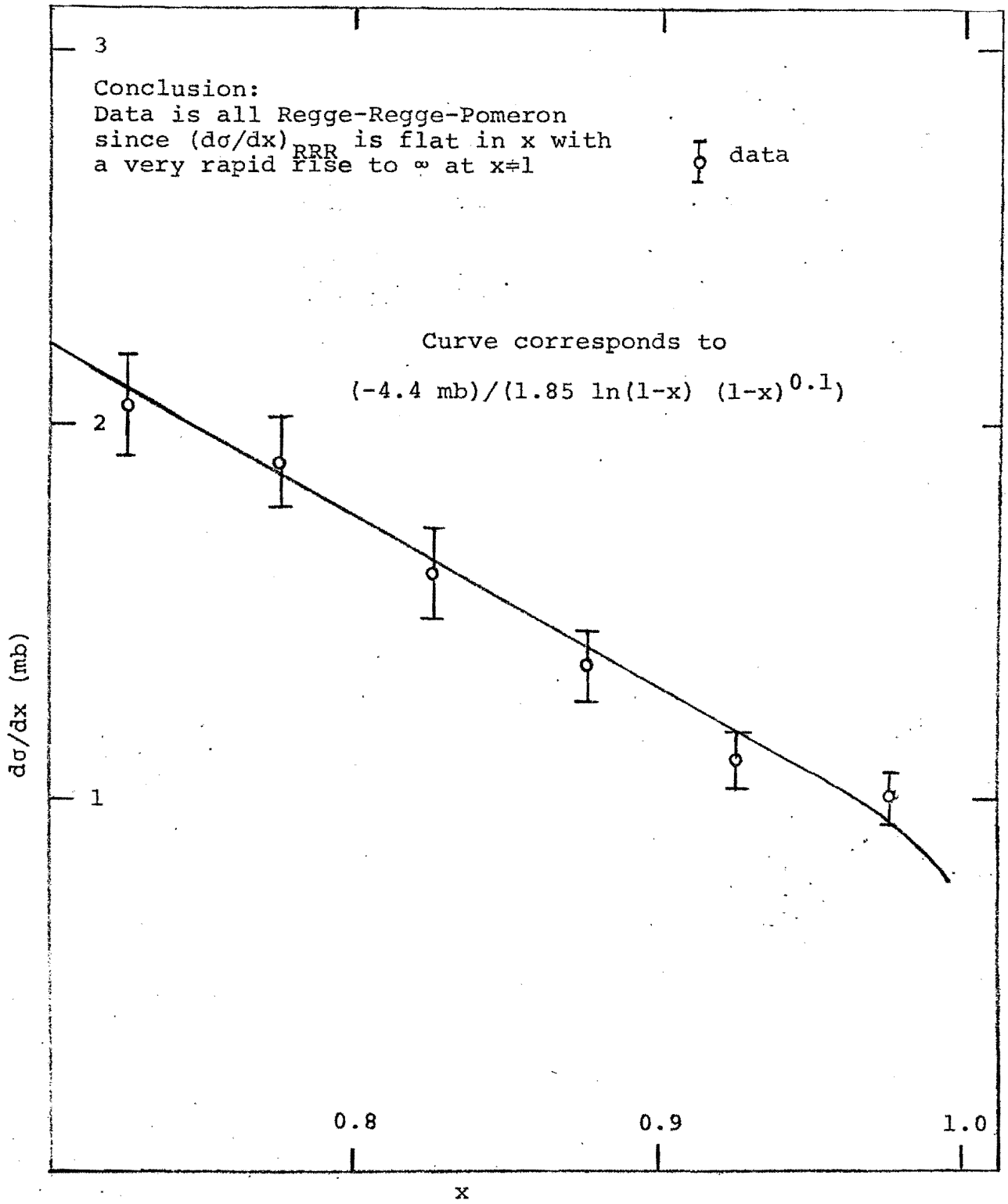

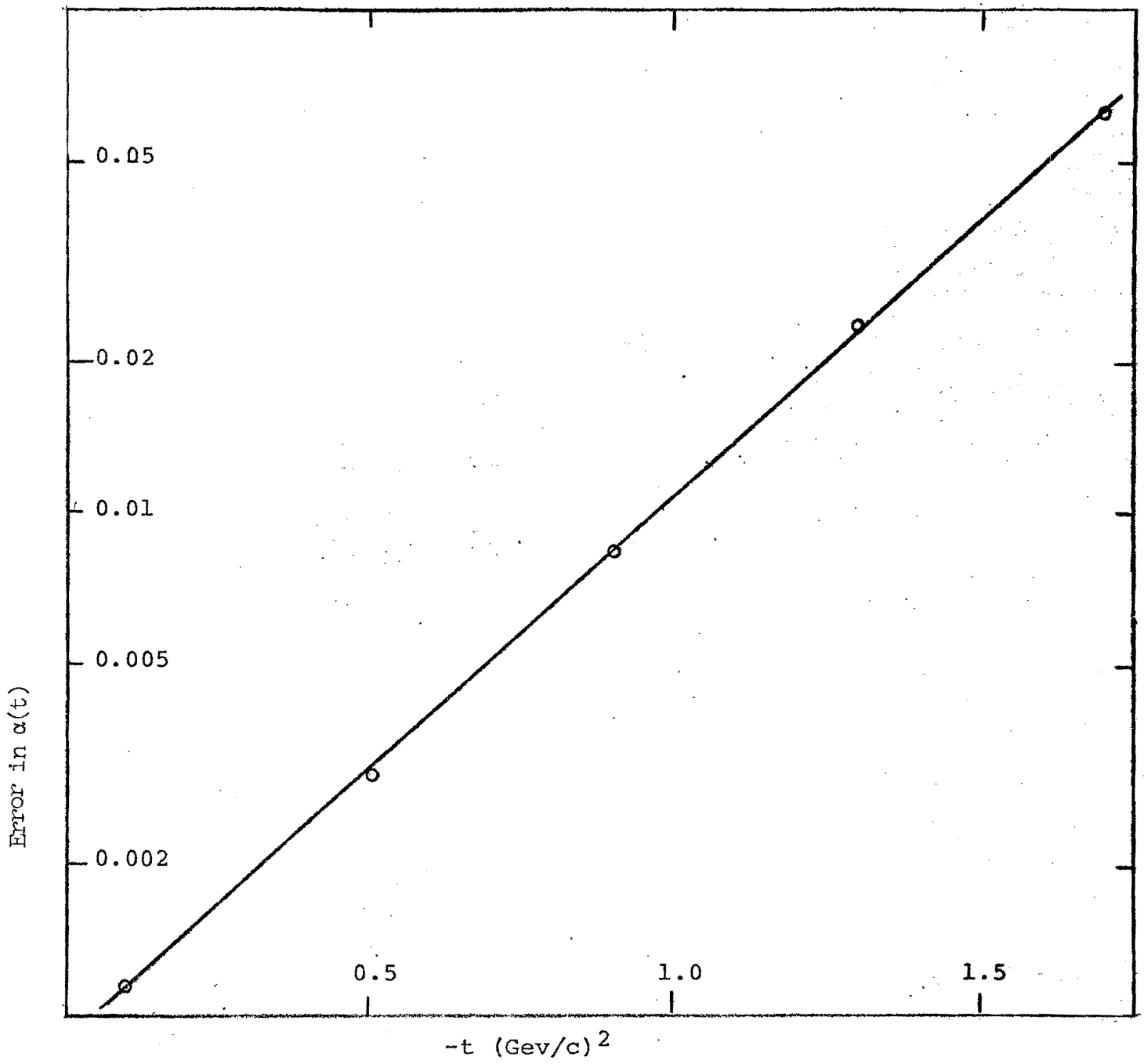

Figure III.

Estimated errors in the measurement of α(t)